ASYMPTOTIC POINCARÉ MAPS ALONG THE EDGES OF POLYTOPES

HASSAN NAJAFI ALISHAH, PEDRO DUARTE, AND TELMO PEIXE

ABSTRACT. For a class of flows on polytopes, including many examples from Evolutionary Game Theory, we describe a piecewise linear model which encapsulates the asymptotic dynamics along the heteroclinic network formed out of the polytope's vertexes and edges. This piecewise linear flow is easy to compute even in higher dimensions, which allows the usage of numeric algorithms to find invariant dynamical structures such as periodic, homoclinic or heteroclinic orbits, which if robust persist as invariant dynamical structures of the original flow. We apply this method to prove the existence of chaotic behavior in some Hamiltonian replicator systems on the five dimensional simplex.

CONTENTS

1. INTRODUCTION

Given a flow on a polytope, leaving all its faces invariant, we call *flowing edge* to any edge of the polytope consisting of a single orbit flowing between the two endpoint singularities. The purpose of this

---

paper is to present a new method to encapsulate and analyze the asymptotic dynamics of the flow along the heteroclinic network formed by the flowing edges and the vertex singularities of the polytope.

Natural examples of such dynamical systems arise in Evolutionary Game Theory (EGT), which was the background motivation for the present work. Even though the phase space of the dynamical systems arising from EGT are usually simplexes or products of simplexes, we state our results in the more general context of simple polytopes in order to have a mathematically comprehensive approach which is also open to new examples.

The replicator equations, introduced by P. Taylor and L. Jonker [20], as well as the polymatrix replicator equation, studied by authors in [1, 2], induce flows on simple polytopes in the scope of applicability of the present results. Polymatrix replicator equations extend the class of bimatrix replicator equations [16, 17].

The use of cross-sections and return maps to analyze dynamics along heteroclinic cycles is an old tool going back to Poincaré. In the context of EGT there is already an extensive literature on the study of boundary heteroclinic cycles [3, 5, 6, 10, 11, 14]. The dynamics along heteroclinic networks has also been widely studied in the context of flows with symmetries [9, Chapter 6]. All these studies use the Poincaré map itself [18, Chapter 6] or its linearization [12, Chapter 17], usually for a bifurcation analysis of families of vector fields. Our method developed to analyze the dynamics along the vertex-edge heteroclinic network is applicable to a wide class of flows on polytopes, with few *apriori* hypothesis on their dynamics. For instance, some of the cumbersome conditions in the previously referenced works can be reformulated in our setting as appropriate assumptions on the (computable) asymptotic dynamics. Moreover, as mentioned below, our method applies to heteroclinic networks with degenerate saddles, in a setting which, as far as we know, is not covered by existing results.

The method presented here was first announced (without proofs) by the second author in [7]. In the following paragraphs, we give an overview of the method.

The Poincaré map defined along a heteroclinic or homoclinic orbit is a composition of two types of maps, the global and the local Poincaré maps. The global ones, P_γ, are defined in tubular neighborhoods of the flowing edges γ, see Figure 1. They map points between two cross sections Σ_γ^- and Σ_γ^+ transversal to the flow along γ. The local ones, P_v, are defined in neighborhoods of vertex singularities v. For any pair of flowing edges γ, γ' such that v is both the endpoint of γ' and the start-point of γ, the local map P_v takes points from $\Sigma_{\gamma'}^+$ to Σ_γ^-.

The nonlinearities of the global Poincaré maps P_γ fade away asymptotically, as one approaches the heteroclinic orbit, becoming identity
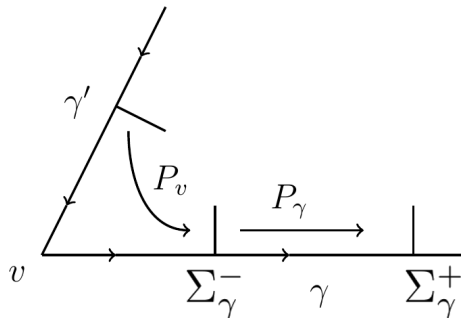
FIGURE 1. The local, P_v, and global, P_γ, Poincaré maps along a heteroclinic orbit.

maps in the limit. Local data is extracted from the underlying vector field X at the vertexes, which will be referred to as the *skeleton character* of X. The asymptotic behavior of the flow is completely determined by this skeleton character and in particular the local Poincaré maps P_v can be asymptotically linearized (in the sense that near the vertexes, trajectories become lines after a change of variables) in terms of this data.

In the generic case, the skeleton character of X at a vertex v consists of the eigenvalues of X along the (eigen) directions of edges through v. The signs of these eigenvalues were used to form the characteristic matrix discussed in [12, Chapter 17]. The skeleton characters considered here are a bit more general. The skeleton character of a *corner* (a vertex v and an edge containing it) may be non-zero even if the associated eigenvalue is zero. This makes the method applicable in certain degenerate situations with many zero eigenvalues. One such example is the compatification of a Hamiltonion Lokta-Voltra system, where all eigenvalues along directions transversal to the facet at infinity vanish [7].

To stage the asymptotic piecewise linear dynamics we introduce a geometric space referred to as the *dual cone* of a polytope. This space is a subset of $\mathbb{R}^F$, where F is the set of the polytope's facets. The dual cone will be a union of sectors[1], one for each vertex of the polytope, see Figure 2. Given a vector field X on a d dimensional polytope $\Gamma^d \subset \mathbb{R}^d$, we describe a rescaling change of coordinates Ψ_ϵ^X, depending on a blow-up parameter ϵ, see Figure 7. This change of coordinates maps tubular neighborhoods of edges and vertexes to the dual cone of Γ^d. For instance, the tubular neighborhood N_v of a vertex v is defined by

$$N_v := \{p \in \Gamma^d : 0 \leq x_j(p) \leq 1 \text{ for } 1 \leq j \leq d\}$$

---

[1] We call sector to any closed convex cone bounded by d transversal facets, where d is the sector's dimension.

where $(x_1, \ldots, x_d)$ is a system of affine coordinates around v which assigns coordinates $(0, \ldots, 0)$ to v and such that the hyperplanes $x_j = 0$ are precisely the facets of the polytope through v. The sets $\{x_j = 0\} \cap N_v$ are referred to as outer facets of N_v. The remaining facets of N_v, defined by equations like $x_i = 1$, are called the inner facets of N_v. The previous cross sections $\Sigma_\gamma^\pm$ are chosen to match these inner facets of the neighborhoods N_v.
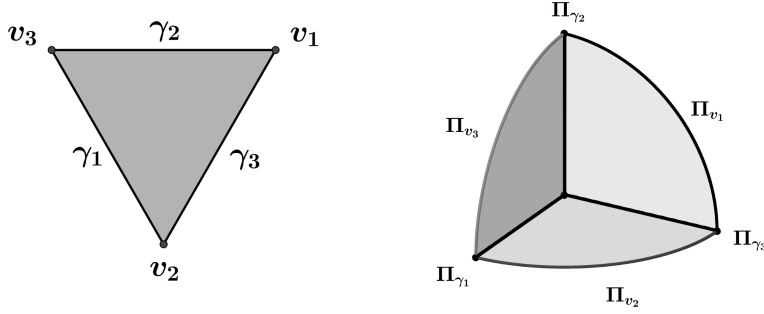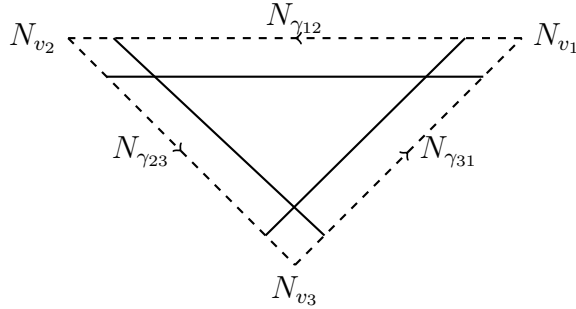

FIGURE 2. Dual cone of a triangle in $\mathbb{R}^F$

FIGURE 3. Tubular neighborhoods along the edges in a two dimensional polytope (dashed lines are the dges)

The rescaling change of coordinates Ψ_ϵ^X takes points in N_v to points in the sector Π_v of all $y = (y_\sigma)_{\sigma \in F} \in \mathbb{R}^F$ with $y_\sigma \geq 0$ and where $y_\sigma = 0$ whenever the facet σ does not contain v. In the generic case, assuming we have enumerated F so that the facets through v are precisely $\sigma_1, \ldots, \sigma_d$, the map Ψ_ϵ^X is defined on the neighborhood N_v by

$$\Psi_\epsilon^X(q) := (-\epsilon^2 \log x_1(q), \ldots, -\epsilon^2 \log x_d(q), 0, \ldots, 0)$$

where $(x_1, \ldots, x_d)$ stand for the system of affine coordinates introduced above. Similarly, given an edge γ, the map Ψ_ϵ^X takes points in the tubular neighborhood N_γ of γ to points in the sector Π_γ of all $(y_\sigma)_{\sigma \in F} \in \mathbb{R}^F$ with $y_\sigma \geq 0$ and where $y_\sigma = 0$ whenever the facet σ does not contain

γ. The map Ψ_ϵ^X sends interior facets of N_v and N_γ, respectively, to boundary facets of Π_v and Π_γ while it takes outer facets of N_v and N_γ to infinity. Figure 3 represents the tubular neighborhoods of vertexes and edges of a triangle, where dashed lines stand for the outer boundary facets of these neighborhoods. Figure 4 depicts the range of the map Ψ_ϵ^X where the dashed lines stand for infinity.
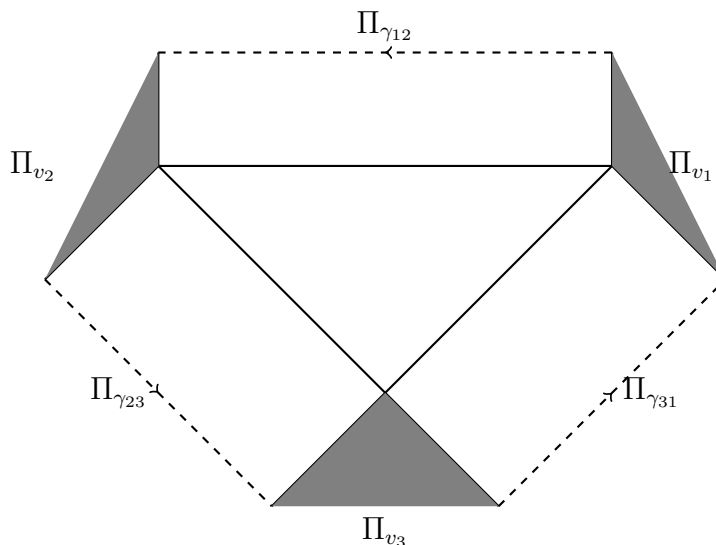

FIGURE 4. Range of the rescaling change of coordinates in the dual cone

As the rescaling parameter ϵ tends to 0, the rescaled push-forward $\epsilon^{-2} (\Psi_\epsilon^X)_* X$ of the vector field X converges to a constant vector field χ^v on each sector Π_v. This means that asymptotically, as $\epsilon \to 0$, trajectories become lines in the coordinates $(y_\sigma)_{\sigma \in F} = \Psi_\epsilon^X$. Given a flowing edge γ between vertexes v and v', the map Ψ_ϵ^X over N_γ depends only on the coordinates transversal to γ. Moreover, as $\epsilon \to 0$ the global Poincaré map P_γ converges to the identity map in the coordinates $(y_\sigma)_{\sigma \in F} = \Psi_\epsilon^X$. Hence the sector Π_γ is naturally identified as the common facet between the sectors Π_v and $\Pi_{v'}$, see Figure 4. In fact, from the above definitions one gets that $\Pi_\gamma = \Pi_v \cap \Pi_{v'}$. Hence the asymptotic dynamics along the vertex-edge heteroclinic network is completely determined by the vector field's geometry near the vertex singularities and can be described by a piecewise constant vector field χ on the dual cone, whose components are precisely those of the skeleton character of X. We refer to this piecewise constant vector field as the *skeleton vector field* of X. This vector field χ induces a piecewise linear flow on the dual cone whose dynamics can be computationally explored.

The flows associated with these piecewise constant vector fields are in general open dynamical systems. Some of them may have no recurrence at all. For instance attracting or repelling vertex singularities, or the existence of attracting or repelling singularities interior to non flowing edges, may divert trajectories and prevent the existence of cycles in the vertex-edge heteroclinic network.

We use Poincaré maps to analyze the asymptotic dynamics of the flow of X. For that we consider a subset S of flowing edges such that every vertex-edge heteroclinic cycle goes through at least one edge in S. We call structural set to any such set S, see Definition 5.8. Then the flow of X induces a Poincaré map P_S on the system of cross sections $\Sigma_S := \cup_{\gamma \in S} \Sigma_\gamma^-$. Each branch of the Poincaré map P_S is associated with a vertex-edge heteroclinic path starting with an edge in S and ending at its first return to another edge in S. These heteroclinic paths are referred to as branches of S. Similarly, the flow of the skeleton vector field χ induces a first return map $\pi_S : D_S \subset \Pi_S \to \Pi_S$ on the system of cross section $\Pi_S := \cup_{\gamma \in S} \Pi_\gamma$ of the dual cone. This map π_S, referred to as the *skeleton flow map*, is piecewise linear and its domain is a finite union of open convex cones, one for each branch of S. Proposition 5.10 provides a simple sufficient condition for the domain D_S of π_S to have full Lebesgue measure in Π_S. In this sense π_S becomes a closed dynamical system. We emphasize that the hypothesis of this proposition is not a requisite for the applicability of our method. Violation of the hypothesis simply allows the existence of open convex cones in $\Pi_S \setminus D_S$ corresponding to orbits which never return to Π_S.

The main result of this manuscript asserts that the Poincaré map P_S in the rescaled coordinates Ψ_ϵ^X converges in the C^∞ topology to the skeleton flow map π_S. More precisely, the following limit holds

$$\lim_{\epsilon \to 0} \Psi_\epsilon^X \circ P_S \circ (\Psi_\epsilon^X)^{-1} = \pi_S$$

with uniform convergence of the map and its derivatives over any compact set contained in the (open) domain $D_S \subset \Pi_S$, see Theorem 6.9.

Consider now, for each facet σ of the polytope, an affine function $\mathbb{R}^d \ni q \mapsto x_\sigma(q) \in \mathbb{R}$ which vanishes on σ and is strictly positive on the rest of the polytope. With this family of affine functions we can present the polytope as $\Gamma^d = \cap_{\sigma \in F}\{x_\sigma \geq 0\}$. In the generic case any function $h : \text{int}(\Gamma^d) \to \mathbb{R}$ of the form

$$h(q) = \sum_{\sigma \in F} c_\sigma \log x_\sigma(q) \quad (c_\sigma \in \mathbb{R})$$

rescales to the following piecewise linear function on the dual cone

$$\eta(y) := \sum_{\sigma \in F} c_\sigma \, y_\sigma$$

in the sense that $\eta = \lim_{\epsilon \to 0} \epsilon^{-2} \left(h \circ (\Psi_\epsilon^X)^{-1}\right)$. When all coefficients c_σ have the same sign then η is a proper function on the dual cone. This

means in particular that all levels of η are compact sets. Finally, if the function h is invariant under the flow of X, i.e., $h \circ P_S = h$ then the piecewise linear function η is also invariant under th skeleton flow, i.e., $\eta \circ \pi_S = \eta$. Thus integrals of motion of conservative systems, which have the previous form, carry over as piecewise linear integrals of the skeleton flow.

As a general principle, any robust structure invariant under the skeleton flow map persists as an invariant structure for the Poincaré map of the original flow. Since the former can be detected through linear algebra tools (e.g. algorithms for computing eigenvalues and eigenvectors of the skeleton flow map's branches) this approach provides a method to analyze the dynamics of the original flow along the vertex-edge heteroclinic network, a method which can be equally well applied to higher dimensional cases. For Hamiltonian systems, to be discussed in a sequel paper, their conservative nature (in the context of Poisson geometry) is inherited by the skeleton flow map. In these cases the analysis of the dynamics reduces to the dimension of the symplectic leaves. We provide here a couple of Hamiltonian examples where this method proves the co-existence of chaotic behavior with elliptic islands.

Embedding the dual cone in the Euclidean space $\mathbb{R}^F$ is formally and computationally convenient. Poincaré maps of the skeleton vector field along paths of the heteroclinic network are represented by $F \times F$ flow matrices on convex cone domains which can be explicitly determined. Both these flow matrices and their convex cone domains are expressed in terms of the vector field's skeleton character.

Next we provide an alternative and more geometric realization of the dual cone as the *normal fan* of a polytope [22, Chapter 7]. A (complete) fan is roughly a family of polyhedral convex closed cones[2] in some Euclidean space $\mathbb{R}^d$ with disjoint interiors and such that their union is the whole space. The *normal cone* of a polytope $\Gamma^d \subset \mathbb{R}^d$ at a vertex v is the closed convex cone

$$\Pi_v := \{u \in \mathbb{R}^d : u \cdot (q - v) \leq 0, \forall\, q \in \Gamma^d\}.$$

The family of all normal cones of a polytope's vertexes (with all their faces) is always a complete fan, referred to as its *normal fan*. Figure 5 shows the normal fan of a triangle in $\mathbb{R}^2$. Given a vertex v of Γ^d let $(x_1, \ldots, x_d)$ be the previously mentioned system of affine coordinates around v. Let $\vec{n}_i \in \mathbb{R}^d$ be the unit outward normal to the facet of Γ^d represented by the equation $x_i = 0$. Then the restriction of the rescaling map Ψ_ϵ^X to the neighborhood N_v with values in the normal

---

[2] The precise definition of fan requires that the intersection of any two family members is either empty of else a common face and that faces of family members are also in the family.

cone Π_v is defined in the generic case by

$$\Psi_\epsilon^X(q) := -\epsilon^2 \sum_{j=1}^{d} \log x_i(q)\, \vec{n}_j.$$

In this construction, the skeleton vector field of X is a piecewise constant vector field on $\mathbb{R}^d$, *i.e.*, one which is constant on each normal cone Π_v for a vertex v of Γ^d.
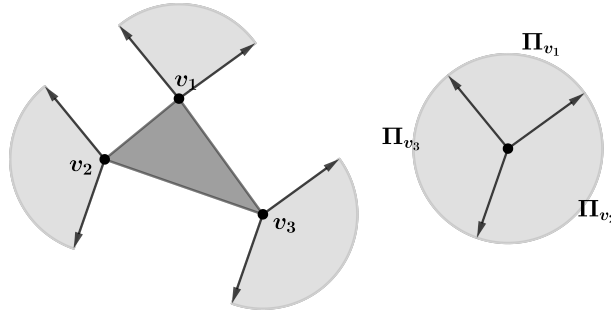
FIGURE 5.   Normal fan of a triangle in $\mathbb{R}^2$.

Figure 6 illustrates a Hamiltonian vector field X (a polymatrix replicator system) on the standard 3-dimensional cube, with a proper Hamiltonian function h. The left of Figure 6 depicts the cube with a few orbits of X on some level set of h. As mentioned above, the function h rescales to a piecewise linear proper function η on the normal fan of the cube. All level sets of η are octahedra (the cube's dual). On the right of Figure 6, a few orbits of the skeleton flow on some level of the invariant function η are shown.

FIGURE 6. Asymptotic linearization on the normal fan

FIGURE 7. Asymptotic linearization on the dual cone

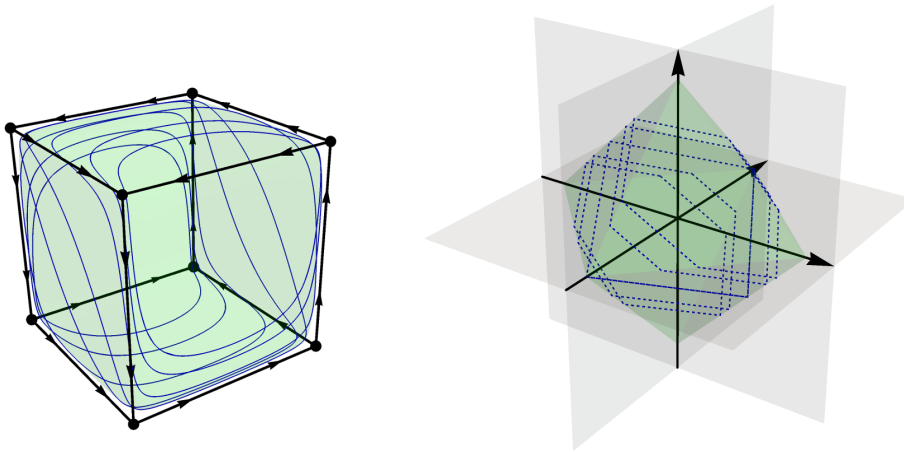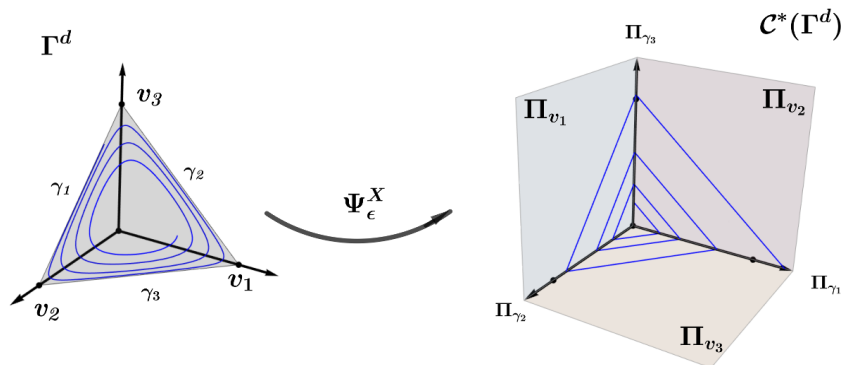All graphics of this manuscript were produced with *Mathematica* and *Geogebra* software. We provide the *Mathematica* code [8] used to analyze the examples and to make the graphics. This code can be used to numerically analyze specific examples, providing hints for analytic results.

This paper is organized as follows. In Section 2 we define polytopes and all their associated notations, terminology and concepts. In Section 3 we introduce the class of vector fields on polytopes, the skeleton character of a vector field and other related concepts. In Section 4, we define the family of rescaling coordinates Ψ_ϵ and the dual cone of a polytope. In Section 5 we introduce the class of skeleton vector fields (piecewise constant vector fields) on the dual cone, whose dynamics encapsulate the asymptotic behavior of the original non-linear flow. We also define the concept of structural set and characterize those vector fields whose skeleton flow map is a closed dynamical system. In Section 6 we define the Poincaré return maps of a vector field, and then state and prove the main thorem, Theorem 6.9. In Section 7 we introduce a probe space of integrals of motion, describing their asymptotics on the dual cone of the polytope. We also describe a sufficient condition on the skeleton flow map for the existence of horse-shes regarding the dynamics of the original vector field, see Theorem 7.8. In Section 8 we summarize a procedure to detect chaotic behavior by checking the assumptions of Theorem 7.8. In Section 9 we describe a couple of replicator Hamiltonian examples in the five dimensional simplex, where the previous procedure is applied. Finally, in Section 10 we discuss a few possible developments of this work.

2. POLYTOPES

In this section we provide preliminary definitions and notations about polytopes.

Given a convex subset $K \subseteq \mathbb{R}^N$, we call *affine support* of K to the the affine subspace spanned by K. The *dimension* of K is by definition the dimension of its affine support.

Definition 2.1. A simple d-dimensional polytope is a compact convex subset $\Gamma^d \subset \mathbb{R}^N$ of dimension d and affine support $E^d \subset \mathbb{R}^N$ for which there exist a family of affine functions $\{f_i : E^d \to \mathbb{R}\}_{i \in I}$, referred to as a defining family of Γ^d, such that

(a) $\Gamma^d = \cap_{i \in I} f_i^{-1}([0, +\infty[)$.
(b) $\Gamma^d \cap f_i^{-1}(0) \neq \emptyset \qquad \forall i \in I$.
(c) Given $J \subseteq I$ such that $\Gamma^d \cap (\cap_{j \in J} f_j^{-1}(0)) \neq \emptyset$, the linear 1-forms $(df_j)_p$ are linearly independent at every point $p \in \cap_{j \in J} f_j^{-1}(0)$.

Given $J \subset I$, because of item (c), if non-empty, the intersection $\Gamma^d \cap (\cap_{j \in J} f_j^{-1}(0))$ is a $(d - |J|)$-dimensional face of the polytope. In particular for each $i \in I$, the set $\sigma_i := \Gamma^d \cap f_i^{-1}(0)$ is a $(d-1)$-dimensional face, *i.e.*, a *facet* of the polytope. We denote the sets of vertexes, edges and facets, respectively, by V, E and F. Since $F = \{\sigma_i : i \in I\} \simeq I$, we will assume from now on that the defining family of Γ^d is indexed in F in a way that $\sigma = \Gamma^d \cap f_\sigma^{-1}(0)$, for all $\sigma \in F$.

Given a vertex v, the sets F_v and E_v are defined to be the set of all facets, respectively edges, which contain v. Since Γ^d is a simple polytope, both these sets have d elements.

Remark 2.2. *By (c) of Definition 2.1 at any given vertex v, the co-vectors $(df_i)_v$ are linearly independent. So in a small enough neighborhood of v the functions $\{f_\sigma\}_{\sigma \in F_v}$ can be used as a system of coordinates.*

Remark 2.3. *We have adopted here the standard terminology where a* polyhedron *is any convex set bounded by finitely many hyperplanes and a* polytope *is a compact polyhedron, see for instance [22]. We note that in [7] the term 'polyhedron' was used to mean compact polyhedron.*

The elements of the set

$$C := \{ (v, \gamma, \sigma) \in V \times E \times F : \gamma \cap \sigma = \{v\} \}$$

are referred to as *corners*, see Figure 8.

Remark 2.4. *Any pair of the elements in a corner uniquely determines the third one. Therefore, we will sometimes refer to the corner (v, γ, σ) shortly as (v, γ) or (v, σ). An edge γ with endpoints v, v' determines two corners (v, γ, σ) and (v, γ, σ'), referred to as the* end corners *of γ. The facets σ, σ' will be referred to as the* opposite facets *of γ.*

Example 2.5. *The d-dimensional simplex is the polytope defined by*

$$\Delta^d := \left\{ (x_0, x_1, \ldots, x_d) : x_j \geq 0, \ \sum_{j=0}^d x_j = 1 \right\}.$$
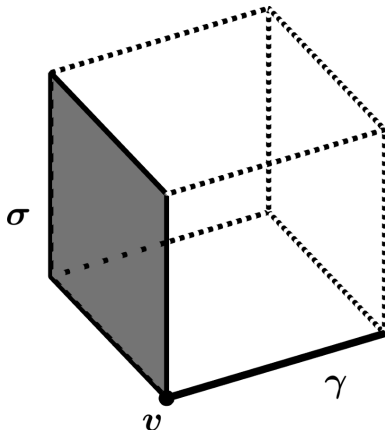
FIGURE 8. A corner (v, γ, σ) in a three dimensional polytope.

The affine support of Δ^d is the hyperplane

$$E^d := \left\{ (x_0, x_1, \ldots, x_d) \in \mathbb{R}^{d+1} : \sum_{j=0}^{d} x_j = 1 \right\}.$$

The defining family of Δ^d are the coordinate functions $f_i : E^d \to \mathbb{R}$, $f_i(x_0, x_1, \ldots, x_d) = x_i$. The simplex Δ^d has $d+1$ vertexes $v_0, v_1, \ldots, v_d$ and $d+1$ facets $\sigma_0, \sigma_1, \ldots, \sigma_d$, where $v_j = (0, \ldots, 1, \ldots, 0)$ is the vertex opposed to the facet $\sigma_j = \Delta^d \cap \{x_j = 0\}$ for each $j = 0, 1, \ldots, d$.

3. Vector Fields on Polytopes

In this section we introduce the general class of vector fields on polytopes to which our theory applies.

Let Γ^d be a simple d-dimensional polytope. A function $f : \Gamma^d \to \mathbb{R}$ is said to be *analytic* if it can be analytically extended to a neighborhood of Γ^d. We denote by $\mathcal{C}^\omega(\Gamma^d)$ the space of all analytic functions on Γ^d. Similarly, we denote by $\mathfrak{X}^\omega(\Gamma^d)$ the space of all analytic vector fields $X : \Gamma^d \to \mathbb{R}^N$ such that for every face $\rho \subset \Gamma^d$ and all $x \in \rho$, the vector $X(x)$ is tangent to ρ. This tangency requirement on the vector fields $X \in \mathfrak{X}^\omega(\Gamma^d)$ implies that for every facet $\sigma \in F$, $df_\sigma(X) = 0$ along σ. By compactness the flow φ_X^t of any vector field $X \in \mathfrak{X}^\omega(\Gamma^d)$ is complete on Γ^d with singularities at the vertexes of the polytope.

Given a vertex v, consider the coordinate system introduced in Remark 2.2, $(x_1, \ldots, x_d) = (f_{\sigma_1}(q), \ldots, f_{\sigma_d}(q))$ where $F_v = \{\sigma_1, \ldots, \sigma_d\}$. In these coordinates the analytic function $df_{\sigma_l}(X)$ vanishes along the hyperplane $x_l = 0$. By Weierstrass division theorem either there exist a positive integer $\nu_l = \nu(X, \sigma_l)$, and the function $H_{\sigma_l} \in \mathcal{C}^\omega(\Gamma^d)$ which is non-identically zero along the face σ_l and such that

$$df_{\sigma_l}(X) = (f_\sigma)^{\nu_l} H_{\sigma_l}, \quad \text{i.e.} \quad \dot{x}_l = x_l^{\nu_l} H_{\sigma_l}, \tag{3.1}$$

or else $df_{\sigma_l}(X)$ is identically zero. In the later case, we set $\nu_l = \infty$. We say that X *has tangency contact of order* $\nu(X, \sigma)$ with σ and will refer to it as the order of X at the facet σ. The map

$$\nu : \mathfrak{X}^\omega(\Gamma^d) \times F \to \{1, 2, 3, \ldots, \infty\}$$

is called *order function* of X.

Remark 3.1. *We have assumed analyticity for the sake of simplicity, also because the EGT models we have in mind are analytic (and even algebraic) vector fields. The results obtained in this work extend easily to smooth flows and vector fields. The main difference is that for a smooth vector field X the concept of order must first be defined locally.*[3]

For every corner (v, σ, γ) there exists a unique vector $e_{(v,\sigma)}$ tangent to γ at v such that $(df_\sigma)_v(e_{(v,\sigma)}) = 1$ and for any other facet $\sigma' \in F_v$, $\sigma' \neq \sigma$, $(df_{\sigma'})_v(e_{(v,\sigma)}) = 0$. Hence, $\{e_{(v,\sigma)}\}_{\sigma \in F_v}$ is the dual basis of the 1-form basis $\{(df_\sigma)_v\}_{\sigma \in F_v}$. The vectors $e_{(v,\sigma)}$ are eigenvectors of the derivative DX_v. If $\nu(X, \sigma) = 1$ then $H_\sigma(v)$ is the eigenvalue of the derivative DX_v associated to $e_{(v,\sigma)}$. In the case $\nu = \nu(X, \sigma) \geq 2$, the eigenvalue associated to $e_{(v,\sigma)}$ is zero but we have

$$H_\sigma(v) = \frac{1}{\nu!}(df_\sigma)_v \, (D^\nu X)_v \big(\underbrace{e_{(v,\sigma)}, \ldots, e_{(v,\sigma)}}_{\nu \text{ times}}\big) \, .$$

To see this consider the coordinate system introduced in Remark 2.2, $(x_1, \ldots, x_d) = (f_{\sigma_1}(q), \ldots, f_{\sigma_d}(q))$, where $F_v = \{\sigma_1, \ldots, \sigma_d\}$. Then the lth component of the vector field X is $X_l(x) = x_l^\nu \, H_{\sigma_l}(x)$ and we have

$$H_{\sigma_l}(v) = \frac{1}{\nu!} \frac{\partial^\nu X_l}{\partial x_l^\nu}(0) = \frac{1}{\nu!}(df_{\sigma_l})_v \, (D^\nu X)_v(e_{(v,\sigma_l)}, \ldots, e_{(v,\sigma_l)}).$$

Definition 3.2. The *skeleton character* of $X \in \mathfrak{X}^\omega(\Gamma^d)$ is defined to be the matrix $\chi := (\chi_\sigma^v)_{(v,\sigma) \in V \times F}$ where

$$\chi_\sigma^v := \begin{cases} -H_\sigma(v) & \sigma \in F_v \\ 0 & \text{otherwise} \end{cases} \, .$$

We set $\chi_\sigma^v = 0$ when $\nu(X, \sigma) = \infty$. For a fixed vertex v, the vector $\chi^v := (\chi_\sigma^v)_{\sigma \in F}$ is referred to as the *skeleton character* at v.

Remark 3.3. *For a given corner (v, γ, σ) if $\chi_\sigma^v < 0$ then v is the α-limit of an orbit in γ, and if $\chi_\sigma^v > 0$ then v is the ω-limit of an orbit in γ. Assuming that X does not have singularities in the interior of an edge γ, if γ connects the corners (v, σ) and (v', σ'), then it consists of a single a heteroclinic orbit with α-limit v and ω-limit v' if and only if $\chi_\sigma^v < 0$ and $\chi_{\sigma'}^{v'} > 0$.*

---

[3] For a smooth vector field X, the order $\nu(X, v, \sigma)$ at a corner (v, σ) is the minimum integer $k \geq 1$ such that $(df_\sigma)_v(D^k X)_v \neq 0$. The order of σ is defined as

$$\nu(X, \sigma) := \min\{\nu(X, v, \sigma) : \sigma \in F_v\} \, .$$

The replicator equation provides a class of analytic vector fields in the space $\mathfrak{X}^\omega(\Delta^d)$. In the rest of this section we recall this equation and describe its skeleton character and order function.

Given a payoff matrix $A \in \mathrm{Mat}_{d+1}(\mathbb{R})$ the system of differential equations

$$\frac{dx_i}{dt} = x_i \left((Ax)_i - \sum_{k=0}^d x_k (Ax)_k \right), \ 0 \le i \le d \qquad (3.2)$$

is called the *replicator equation*. The associated vector field X_A is called the *replicator vector field* of A and lies in our class, $X_A \in \mathfrak{X}^\omega(\Delta^d)$. For a brief interpretation of this equation consider a population whose individuals interact with each other according to the set of pure strategies $\{0, \dots, d\}$. A point $x = (x_0, \dots, x_d) \in \Delta^d$ represents a state of the population where x_i measures the frequency of usage of strategy i. Each entry a_{ij} of A represents the payoff of strategy i against j and this model governs the time evolution of the frequency distribution of each pure strategy. The equation says that the growth rate of each frequency x_i is the difference between its payoff $(Ax)_i = \sum_{j=0}^d a_{ij} x_j$ and the average population's payoff $\sum_{k=0}^d x_k (Ax)_k$.

The next proposition characterizes the skeleton character of X_A.

Proposition 3.4. *Given $A \in \mathrm{Mat}_{d+1}(\mathbb{R})$, every facet σ_i of Δ^d has order 1, 2 or ∞. More precisely*

(1) *$\nu(X_A, \sigma_i) = 1$ iff $a_{ij} \ne a_{jj}$ for some j or else $(a_{kj} - a_{jj})_{k,j \ne i}$ is not skew-symmetric. In this case $\chi_{\sigma_i}^{v_j} = a_{jj} - a_{ij}$ for all j.*

(2) *$\nu(X_A, \sigma_i) = 2$ iff $a_{ij} = a_{jj}$ for all j and $(a_{kj} - a_{jj})_{k,j \ne i}$ is skew-symmetric, but $(a_{kj} - a_{jj})_{k,j}$ is not skew-symmetric. In this case $\chi_{\sigma_i}^{v_j} = a_{ji} - a_{ii}$ for all j.*

(3) *$\nu(X_A, \sigma_i) = \infty$ iff $a_{ij} = a_{jj}$ for all j and $(a_{kj} - a_{jj})_{k,j}$ is skew-symmetric. In this case $\chi_{\sigma_i}^{v_j} = 0$ for all j.*

Proof. Consider the conditions

(C1) $a_{ij} \ne a_{jj}$ for some j or else $(a_{kj} - a_{jj})_{k,j \ne i}$ is not skew-symmetric.

(C2) $a_{ij} = a_{jj}$ for all j and $(a_{kj} - a_{jj})_{k,j \ne i}$ is skew-symmetric, but $(a_{kj} - a_{jj})_{k,j}$ is not skew-symmetric.

(C3) $a_{ij} = a_{jj}$ for all j and $(a_{kj} - a_{jj})_{k,j}$ is skew-symmetric.

It is clear that (C1), (C2) and (C3) are exhaustive and mutually exclusive conditions. Hence it is enough to prove that (C1) $\Rightarrow \nu(X_A, \sigma_i) = 1$, (C2) $\Rightarrow \nu(X_A, \sigma_i) = 2$ and (C3) $\Rightarrow \nu(X_A, \sigma_i) = \infty$.

Let $H_i : \Delta^d \to \mathbb{R}$ be the function

$$H_i(x) := (Ax)_i - \sum_{k=0}^d x_k (Ax)_k.$$

A simple computation shows that

$$H_i(v_j) = a_{ij} - a_{jj}$$

where the v_j are the vertexes of Δ^d. Thus, if for some j, $a_{ij} \neq a_{jj}$ then $\nu(X_A, \sigma_i) = 1$ and $\chi_{\sigma_i}^{v_j} = a_{jj} - a_{ij}$ for all j. Assume now that (C1) holds and let $\tilde{A} = (a_{kj} - a_{jj})_{k,j}$. Then $H_i(x) = (\tilde{A}x)_i - \sum_{k=0}^{d} x_k (\tilde{A}x)_k$. If $a_{ij} = a_{jj}$ for all j then $(\tilde{A}x)_i = 0$ for all $x \in \Delta^d$. Also, if $a_{ij} = a_{jj}$ for all j then the matrix $(\tilde{a}_{kj})_{k,j\neq i}$ is not skew-symmetric. This implies that the closed cone C_i defined by the conditions $x_i = 0$ and $x^T \tilde{A} x = 0$ has zero Lebesgue measure in the hyperplane $\{x_i = 0\} \subset \mathbb{R}^{d+1}$. Therefore $C_i \cap \sigma_i$ has zero Lebesgue measure in the facet σ_i, which implies that $H_i(x) = -x^T \tilde{A} x$ is not identically zero on σ_i. Hence $\nu(X_A, \sigma_i) = 1$ and $\chi_{\sigma_i}^{v_j} = -H_i(v_j) = a_{jj} - a_{ij} = 0$ for all j.

Assuming (C2) holds we have $(\tilde{A}x)_i = 0$ and

$$H_i(x) = -x^T \tilde{A} x = -x_i \sum_{j=0}^{d} (a_{ji} - a_{ii}) \, x_j.$$

Because $(a_{kj} - a_{jj})_{k,j}$ is not skew-symmetric we have $a_{ji} \neq a_{ii}$ for some j. Thus $\nu(X_A, \sigma_i) = 2$ and $\chi_{\sigma_i}^{v_j} = a_{ji} - a_{ii}$ in this case.

Finally, if (C3) holds then $H_i \equiv 0$, which implies $\nu(X_A, \sigma_i) = \infty$. $\quad\square$

4. Rescaling Coordinates

In this section we define the dual cone of a polytope and introduce the family of rescaling coordinates Ψ_ϵ^X described in the introduction.

Consider a polytope Γ^d and its defining family $\{f_\sigma\}_{\sigma \in F}$, see Definition 2.1. By Remark 2.2, the co-vectors $\{(df_\sigma)_v : \sigma \in F_v\}$ are linearly independent at every vertex v. Multiplying each affine function of this family by some large positive number we may assume that the neighborhoods

$$N_v := \{q \in \Gamma^d : \ f_\sigma(q) \leq 1, \ \forall \sigma \in F_v\},$$

with $v \in V$, are pairwise disjoint, and that the functions $\{f_\sigma : \sigma \in F_v\}$ define a coordinate system for Γ^d on N_v. For any edge γ connecting two vertexes $v, v' \in V$ we can define a tubular neighborhood connecting N_v to $N_{v'}$ by

$$N_\gamma := \{q \in \Gamma^d \backslash (N_v \cup N_{v'}) : f_\sigma(q) \leq 1 \text{ for all } \gamma \subset \sigma\}.$$

As before, we may assume that these neighborhoods are pairwise disjoint between themselves. Furthermore, fixing a smooth submersion $t : \overline{N_\gamma} \to [0, 1]$ such that $t^{-1}(0) \subset \partial N_v$ and $t^{-1}(1) \subset \partial N_{v'}$, whose restriction induces a diffeomorphism between $\gamma \setminus \text{int}(N_v \cup N_{v'})$ and $[0, 1]$, the family of functions $\{t, \{f_\sigma\}_{\gamma \subset \sigma}\}$ defines a coordinate system for the polytope on N_γ. The edge skeleton's tubular neighborhood

$$N_{\Gamma^d} := (\cup_{v \in V} N_v) \cup (\cup_{\gamma \in E} N_\gamma) \tag{4.1}$$

will be the domain of our rescaling maps Ψ_ϵ^X, see Figure 3.

Remark 4.1. *We can turn the previous local coordinate systems over the neighborhoods N_v and N_γ into a global system of coordinates over N_{Γ^d} with values in $\mathbb{R}^F$ as follows:*

Each point $q \in N_v$ has coordinates $x = (x_\sigma)_\sigma \in \mathbb{R}^F$, where $x_\sigma = f_\sigma(q)$ if $v \in \sigma$ and $x_\sigma = 0$ otherwise.

Similarly, a point $q \in N_\gamma$ has coordinates $x = (x_\sigma)_\sigma \in \mathbb{R}^F$, where $x_\sigma = f_\sigma(q)$ if $\gamma \subset \sigma$ and $x_\sigma = 0$ otherwise. Note that we have dropped the coordinate $t = t(q)$ and hence this 'coordinate system' fails to be injective. The missing coordinate will not really matter because, as explained in the introduction, global Poincaré maps become identity maps asymptotically.

We use the following family of functions to define the rescaling coordinates. For every $n = 1, 2, \ldots$, let $h_n : (0, 1] \to \mathbb{R}$ be the function

$$h_1(x) = -\log x \quad \text{and} \quad h_n(x) = -\frac{1}{n-1}\left(1 - \frac{1}{x^{n-1}}\right) \quad n \geq 2. \quad (4.2)$$

Remark 4.2. *This family is characterized by the properties:*
$h_n'(x) = -x^{-n}$, $h_n(0) = +\infty$ *and* $h_n(1) = 0$, *which imply that the function* $h_n : (0, 1] \to [0, +\infty)$ *is a diffeomorphism. A straightforward computation yields*

$$(h_1)^{-1}(y) = e^{-y} \text{ and } (h_n)^{-1}(y) = (1 + (n-1)y)^{-\frac{1}{n-1}} \text{ if } n \geq 2.$$

Definition 4.3. Given $X \in \mathfrak{X}^\omega(\Gamma^d)$ we define the ϵ-rescaling coordinate system $\Psi_\epsilon^X : N_{\Gamma^d} \setminus \partial\Gamma^d \to \mathbb{R}^F$ which maps $q \in N_{\Gamma^d}$ to $y := (y_\sigma)_{\sigma \in F}$ where

- if $q \in N_v$ for some vertex v:
$$y_\sigma = \begin{cases} \epsilon^2 h_{\nu(X,\sigma)}(f_\sigma(q)) & \text{if} \quad \sigma \in F_v \\ 0 & \text{if} \quad \sigma \notin F_v \end{cases}$$

- if $q \in N_\gamma$ for some edge γ:
$$y_\sigma = \begin{cases} \epsilon^2 h_{\nu(X,\sigma)}(f_\sigma(q)) & \text{if} \quad \gamma \subset \sigma \\ 0 & \text{if} \quad \gamma \not\subset \sigma \end{cases}$$

For a given vertex $v \in V$ we define
$$\Pi_v := \left\{ (y_\sigma)_{\sigma \in F} \in \mathbb{R}_+^F : y_\sigma = 0 \quad \forall \sigma \notin F_v \right\}. \quad (4.3)$$

Since $\{f_\sigma : \sigma \in F_v\}$ is a coordinate system for Γ^d in N_v and the functions $h_n : (0, 1] \to [0, +\infty)$ are diffeomorphisms, the restriction of Ψ_ϵ^X to $N_v \setminus \partial\Gamma^d$ is a diffeomorphism onto Π_v.

Next consider an edge γ connecting two corners (v, σ) and (v', σ'). Note that $F_v \cap F_{v'} = \{\sigma \in F : \gamma \subset \sigma\}$, which means that the image

$$\Psi_\epsilon^X(N_\gamma \setminus \partial\Gamma^d) = \left\{ (y_\sigma)_{\sigma \in F} \in \mathbb{R}_+^F : y_\sigma = 0 \quad \text{when } \gamma \not\subset \sigma \right\}.$$

is equal to $\Pi_v \cap \Pi_{v'}$. We denote this image by Π_γ. Notice that N_γ has dimension d, while Π_γ has dimension $d - 1$. In particular the map Ψ_ϵ^X is not injective over N_γ.

Let us explain the use of the term 'coordinate system' here. As mentioned above, the family of functions $\{t, \{f_\sigma\}_{\gamma \subset \sigma}\}$ defines a coordinate system for Γ^d on $\overline{N_\gamma}$. For any $t_0 \in (0, 1)$, let $\Sigma_{t_0} := \{q \in N_\gamma : t(q) = t_0\}$. This set is a transversal cross-section to γ at the point $q = \gamma \cap t^{-1}(t_0)$. Between the boundary transversal cross-sections Σ_0, Σ_1, we have

$$\Psi_\epsilon^X(\Sigma_t) = \Psi_\epsilon^X(N_\gamma) \quad \forall t \in [0, 1].$$
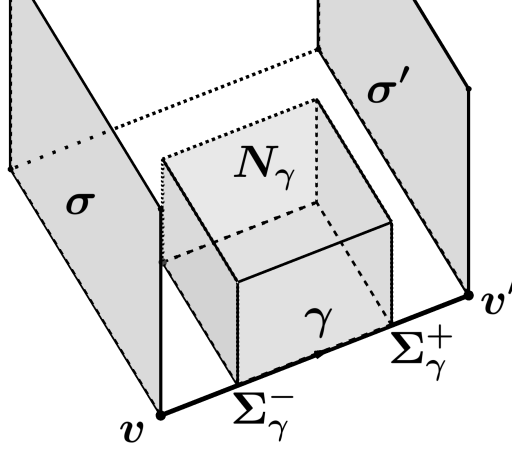

FIGURE 9. An edge connecting two corners

As mentioned in the introduction, asymptotically the global Poincaré maps are identity maps, see Lemma (6.2). Thus the asymptotic flow identifies all cross-sections Σ_t, $t \in [0, 1]$. This makes the map Ψ_ϵ^X a suitable 'coordinate system' for our purposes.

Definition 4.4. The *dual cone* of Γ^d is defined to be

$$\mathcal{C}^*(\Gamma^d) := \bigcup_{v \in V} \Pi_v \,,$$

where Π_v is the sector defined at (4.3). Points of the dual cone will always be denoted by $y = (y_\sigma)_{\sigma \in F}$.

By construction, the dual cone is the range of the ϵ-rescaling coordinate system, *i.e.*, $\Psi_\epsilon^X(N_{\Gamma^d} \setminus \partial \Gamma^d) = \mathcal{C}^*(\Gamma^d)$. In particular these coordinates determine a family of maps $\Psi_\epsilon^X : N_{\Gamma^d} \setminus \partial \Gamma^d \to \mathcal{C}^*(\Gamma^d)$. We will write $\Psi_{v,\epsilon}^X$ instead of Ψ_ϵ^X to emphasize that we are dealing with the restriction of the ϵ-rescaling coordinates to the neighborhood N_v, which is a diffeomorphism $\Psi_{v,\epsilon}^X : N_v \setminus \partial \Gamma^d \to \Pi_v$.

To explain the term 'dual' notice first that $\Pi_\gamma = \Pi_v \cap \Pi_{v'}$, whenever γ is an edge connecting the vertexes v and v'. Similar relations hold for higher dimensional faces. In fact for any face $\rho \subset \Gamma^d$, we can define

$$\Pi_\rho := \{ (y_\sigma)_{\sigma \in F} \in \mathbb{R}_+^F : y_\sigma = 0 \quad \text{when } \rho \not\subset \sigma \}.$$

The dual cone $\mathcal{C}^*(\Gamma^d)$ has a simplicial structure where Π_ρ is a face of $\mathcal{C}^*(\Gamma^d)$ for every face ρ of Γ^d. Moreover, for any faces ρ, ρ' of Γ^d,

$$\rho \subset \rho' \quad \Leftrightarrow \quad \Pi_{\rho'} \subset \Pi_\rho.$$

The dual cone of a polytope can be identified with the polytope's normal fan, which in turn coincides with the face fan of its dual polytope, see [22, Chapter 7]. This gives a short explanation for the inherent duality between a polytope and its dual cone.

The following technical lemma will be used to control the asymptotic behavior of Ψ_ϵ^X.

Lemma 4.5. *For any $n \geq 1$ and $k \geq 1$, there exists $0 < r(k, n) \leq 1$ such that the diffeomorphisms $h_n : (0, 1] \to [0, +\infty)$ satisfy*

(1) $\displaystyle \lim_{\epsilon \to 0^+} \max_{0 \leq i \leq k} \sup_{y \geq \epsilon^r} \left| \frac{d^i}{dy^i} h_n^{-1} \left(\frac{y}{\epsilon^2} \right) \right| = 0,$

(2) $\displaystyle \lim_{\epsilon \to 0^+} \max_{0 \leq i \leq k} \sup_{y \geq \epsilon^r} \left| \frac{d^i}{dy^i} \left[\epsilon^2 \left(h_l \circ (h_n)^{-1} \right) \left(\frac{y}{\epsilon^2} \right) \right] \right| = 0 \quad \text{for } 1 \leq l < n.$

Moreover $r(k, 1) = 1$ for all $k \geq 1$.

Proof. For $n = 1$ take $r = 1$ regardless of k. The kth derivative of e^{-y/ϵ^2} is bounded, over $y \geq \epsilon$, by $\epsilon^{-2k} e^{-1/\epsilon}$, which tends to 0 as $\epsilon \to 0^+$. In this case the conclusion (2) is empty.

For $n > 1$ and $y \geq \epsilon^r$ the kth derivative of $h_n^{-1}(y/\epsilon^2)$ is bounded by

$$\frac{(n-1)^k}{\epsilon^{2k}} \prod_{j=0}^{k-1} \left(-\frac{1}{n-1} - j \right) \left(1 + \frac{\epsilon^r}{\epsilon^2} \right)^{-\frac{1}{n-1}-k} \asymp \epsilon^{(2-r)(\frac{1}{n-1}+k)-2k}$$

$$= \epsilon^{\frac{2}{n-1} - r(\frac{1}{n-1}+k)}$$

which tends to 0 as $\epsilon \to 0^+$, provided we choose

$$0 < r < \frac{\frac{2}{n-1}}{\frac{1}{n-1} + k} = \frac{2}{1 + (n-1)k} \leq 1.$$

The last inequality holds for any $n \geq 2$. This proves item (1).

Consider now the family of functions $g_l(\epsilon, y) := \epsilon^2 (h_l \circ h_n^{-1})(y/\epsilon^2)$ with $1 \leq l < n$. For $l = 1$ we have

$$g_1(\epsilon, y) = \frac{\epsilon^2}{n-1} \log \left(1 + (n-1) \frac{y}{\epsilon^2} \right)$$

and over the interval $y \geq \epsilon^r$, $g_1(\epsilon, y) = \mathcal{O}(\epsilon)$ as $\epsilon \to 0$. The higher order derivatives of $g_1(\epsilon, y)$ are

$$\frac{d^k g_1}{dy^k}(\epsilon, y) = \pm (k-1)! \left(\frac{n-1}{\epsilon} \right)^{k-1} \left(1 + (n-1) \frac{y}{\epsilon^2} \right)^{-k}.$$

Hence over the interval $y \geq \epsilon^r$

$$\frac{d^k g_1}{dy^k}(\epsilon, y) = \mathcal{O}(\epsilon^{2-rk}) \quad \text{as} \quad \epsilon \to 0$$

and this tends to 0 provided $r < \frac{2}{k}$.

For $2 \leq l < n$ set $\theta_l = \frac{l-1}{n-1}$ and notice that $\theta_l < \frac{n-2}{n-1} < 1$. A simple calculation gives

$$g_l(\epsilon, y) = -\frac{\epsilon^2}{l-1} + \frac{\epsilon^2}{l-1}\left(1 + (n-1)\frac{y}{\epsilon^2}\right)^{\theta_l}$$

and over the interval $y \geq \epsilon^r$ one has $g_l(\epsilon, y) = \mathcal{O}(\epsilon^{\frac{2}{n-1}})$ as $\epsilon \to 0$. For $k \geq 1$, the higher order derivatives of $g_l(\epsilon, y)$ are

$$\frac{d^k g_l}{dy^k}(\epsilon, y) = \pm\frac{n-1}{l-1}\left[\prod_{j=0}^{k-1}(\theta_l - j)\right]\left(\frac{n-1}{\epsilon^2}\right)^{k-1}\left(1 + (n-1)\frac{y}{\epsilon^2}\right)^{\theta_l - k}.$$

Hence over the interval $y \geq \epsilon^r$

$$\frac{d^k g_l}{dy^k}(\epsilon, y) = \mathcal{O}(\epsilon^{-r(k-\frac{n-2}{n-1})+\frac{2}{n-1}}) \quad \text{as} \quad \epsilon \to 0$$

which tends to 0 provided $r < \frac{2}{k(n-1)-(n-2)}$. This proves item (2). $\square$

To shorten statements about convergence in the forthcoming lemmas and theorems we introduce some terminology.

Definition 4.6. Suppose we are given a family of functions F_ϵ with varying domains $\mathscr{D}_\epsilon$. Let F be another function with domain $\mathscr{D}$. Assume that all these functions have the same target and source spaces, which are assumed to be linear spaces. We will say that $\lim_{\epsilon \to 0^+} F_\epsilon = F$ *in the C^k topology*, to mean that:

(1) *domain convergence*: for every compact subset $K \subseteq \mathscr{D}$, we have $K \subseteq \mathscr{D}_\epsilon$ for every small enough $\epsilon > 0$, and

(2) *uniform convergence on compact sets*:

$$\lim_{\epsilon \to 0^+} \max_{0 \leq i \leq k} \sup_{u \in K} \left| D^i\left[F_\epsilon(u) - F(u)\right] \right| = 0.$$

Convergence in the C^∞ topology means convergence in the C^k topology for all $k \geq 1$. If in a statement F_ϵ is a composition of two or more mappings then its domain should be understood as the composition domain.

Next lemma relates the asymptotic push-forward of X by Ψ_ϵ^X near a vertex v with the skeleton character χ^v of X at v, see Definition 3.2. It says that the vector field $(\Psi_\epsilon^X)_* X$ rescaled by the factor ϵ^{-2} converges to the constant vector field χ^v on the sector Π_v. In particular the trajectories of the push-forward vector field $(\Psi_\epsilon^X)_* X$ are asymptotically linearized to the lines of the flow of the constant vector field χ^v. We will denote by $\Psi_{v,\epsilon}^X$ the restriction of Ψ_ϵ^X to N_v. Define also

$$\Pi_v(\epsilon) := \{ y \in \Pi_v : y_\sigma \geq \epsilon \quad \text{for all} \quad \sigma \in F_v \} \tag{4.4}$$

Lemma 4.7. *Consider the functions H_σ defined in (3.1). Then*

$$(\Psi_{v,\epsilon}^X)_* X = \epsilon^2 \left(\tilde{X}_{v,\sigma}^\epsilon \right)_{\sigma \in F},$$

where

$$\tilde{X}_{v,\sigma}^\epsilon(y) := \begin{cases} -H_\sigma \left((\Psi_{v,\epsilon}^X)^{-1}(y) \right) & if \ \sigma \in F_v \\ 0 & if \ \sigma \notin F_v \end{cases}.$$

Moreover, given $k \geq 1$ there exists $r = r(k,X) > 0$ such that the following limit holds in the C^k topology

$$\lim_{\epsilon \to 0} (\tilde{X}_v^\epsilon)|_{\Pi_v(\epsilon^r)} = \chi^v .$$

Proof. Let $F_v = \{\sigma_1, \ldots, \sigma_d\}$ and $(x_1, \ldots, x_d) = (f_{\sigma_1}(q), \ldots, f_{\sigma_d}(q))$ be the coordinate system introduced in Remark 2.2. Denote by ν_l the order of the facet σ_l. Let $H_l(x)$ be the function $H_{\sigma_l}(q)$ expressed in this coordinate system. Then by (3.1), the equation $\frac{dq}{dt} = X(q)$ is equivalent to the system of differential equations

$$\frac{dx_l}{dt} = x_l^{\nu_l} H_l(x), \quad 1 \leq l \leq d .$$

In these coordinates

$$\Psi_{v,\epsilon}^X(x_1, \ldots, x_d) = \epsilon^2 \left(h_{\nu_1}(x_1), \ldots, h_{\nu_d}(x_d), 0, \ldots, 0 \right).$$

Therefore, since the Jacobian of $\Psi_{v,\epsilon}^X$ can be identified with the diagonal matrix

$$D(\Psi_{v,\epsilon}^X)_x = -\epsilon^2 \mathrm{diag}(x_1^{-\nu_1}, \ldots, x_d^{-\nu_d})$$

the first claim follows.

Fix $k \in \mathbb{N}$ and take $r = \min_{1 \leq j \leq d} r(k, \nu_j)$,, where $r(k,n)$ is tha function in Lemma 4.5. Given $y \in \Pi_v(\epsilon^r)$,

$$H_{\sigma_l} \left((\Psi_{v,\epsilon}^X)^{-1}(y) \right) = H_l \left(h^{-1}(\frac{y}{\epsilon^2}) \right),$$

where $h^{-1}(\frac{y}{\epsilon^2}) := \left(h_{\nu_1}^{-1}(\epsilon^{-2} y_{\sigma_1}), \ldots, h_{\nu_d}^{-1}(\epsilon^{-2} y_{\sigma_d}) \right)$. Thus, by item (1) of Lemma 4.5 combined with Definition 3.2, the convergence follows. $\square$

5. Skeleton Vector Fields

In this section we define the skeleton of a vector field $X \in \mathfrak{X}^\omega(\Gamma^d)$ and its corresponding skeleton flow map, explaining how it is computed and its dynamics is analyzed.

Definition 5.1. Given $X \in \mathfrak{X}^\omega(\Gamma^d)$, the *skeleton* of X is the piecewise constant vector field χ on dual cone $\mathcal{C}^*(\Gamma^d)$ which is constant and equal to χ^v on each sector Π_v, where $\chi^v = (\chi_\sigma^v)_{\sigma \in F}$ is the skeleton character at v introduced in Definition 3.2. Notice that for every vertex v, the vector χ^v is tangent to Π_v.

Our goal is to study the piecewise linear flow generated by the skeleton vector field χ. Remark 3.3 justifies that we call χ-*repelling* a vertex v such that $\chi_\sigma^v < 0$, $\forall \sigma \in F_v$, and χ-*attractive* if $\chi^v > 0$, $\forall \sigma \in F_v$. A vertex v is said to be of *saddle type* if for some pair of facets $\sigma_1, \sigma_2 \in F$ one has $\chi_{\sigma_1}^v \chi_{\sigma_2}^v < 0$. The edges of Γ^d are also classified as follows.

Definition 5.2. Let $\gamma \in E$ be an edge with end corners (v, σ) and (v', σ'). We say that γ is a *defined type edge* if either $\chi_\sigma^v \chi_{\sigma'}^{v'} \neq 0$ or else $\chi_\sigma^v = \chi_{\sigma'}^{v'} = 0$. A defined type edge γ is called

(1) a *flowing-edge* if $\chi_\sigma^v \chi_{\sigma'}^{v'} < 0$,
(2) a *neutral edge* if $\chi_\sigma^v = \chi_{\sigma'}^{v'} = 0$,
(3) an *attracting edge* if $\chi_\sigma^v < 0$ and $\chi_{\sigma'}^{v'} < 0$,
(4) a *repelling edge* if $\chi_\sigma^v > 0$ and $\chi_{\sigma'}^{v'} > 0$,

For a flowing-edge γ with opposite corners (v, σ) and (v', σ'), we write $(v, \sigma) \xrightarrow{\gamma} (v', \sigma')$, whenever $\chi_\sigma^v < 0$ and $\chi_{\sigma'}^{v'} > 0$. The vertexes v and v' are respectively called the *source* of γ, denoted by $s(\gamma)$, and the *target* of γ, denoted by $t(\gamma)$.

We call *orbit* of χ to any continuous piecewise affine function $c : I \to \mathcal{C}^*(\Gamma^d)$, defined on some interval $I \subset \mathbb{R}$, such that

(1) $c'(t) = \chi^v$ whenever $c(t)$ is interior to some Π_v, with $v \in V$,
(2) there is at most a countable set of times $t \in I$ such that $c(t)$ is not interior to any sector Π_v, with $v \in V$.

Writing $I = [t_0, t_n]$, a sequence of vertexes $(v_1, v_2, \ldots, v_m)$ such that for some times $t_0 < t_1 < \ldots < t_{n-1} < t_n$ one has $c(t) \in \text{int}(\Pi_{v_j})$ for all $t_{j-1} < t < t_j$, is called the *itinerary* of the orbit segment c. This implies that $c(t_j) \in \Pi_{v_{j-1}} \cap \Pi_{v_j} = \Pi_\gamma$, where $v_{j-1} \xrightarrow{\gamma} v_j$ is a flowing edge, for every $j = 1, \ldots, n-1$. If there are flowing edges γ_0 and γ_n such that the endpoints satisfy $c(t_0) \in \Pi_{\gamma_0}$ and $c(t_n) \in \Pi_{\gamma_n}$ then the sequence of edges $(\gamma_0, \gamma_1, \ldots, \gamma_n)$ is also referred to as the *itinerary* of the orbit segment c.

Definition 5.3. We say that a vector field $X \in \mathfrak{X}^\omega(\Gamma^d)$ is *regular* when all its edges have defined type and

(1) X has no singularities in $\text{int}(\gamma)$ for every flowing edge γ,
(2) X vanishes along every neutral edge γ.

From now on, we will only consider regular vector fields. Figure 10 depicts the relation between the orientation of the flow of X along γ and the orientation of the flow of χ around Π_γ.

Given vertex v of saddle type together with an incoming flowing-edge $v_* \xrightarrow{\gamma} v$ and an outgoing flowing-edge $v \xrightarrow{\gamma'} v'$, denoting by σ_* the facet opposed to γ' at v we define the sector $\Pi_{\gamma, \gamma'} = \Pi_{\gamma, \gamma'}^\chi$

$$\Pi_{\gamma, \gamma'} := \left\{ y \in \text{int}(\Pi_\gamma) : y_\sigma - \frac{\chi_\sigma^v}{\chi_{\sigma_*}^v} y_{\sigma_*} > 0, \forall \sigma \in F_v, \sigma \neq \sigma_* \right\} \quad (5.1)$$
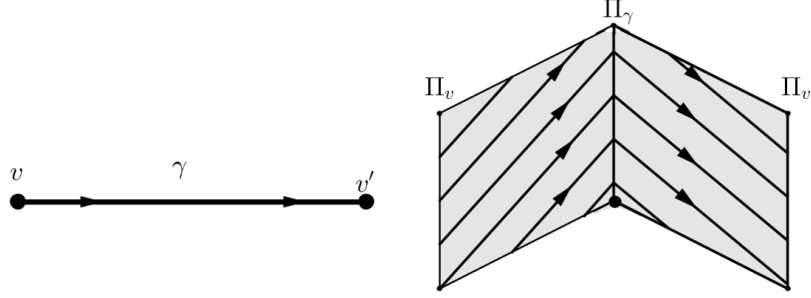
FIGURE 10. A flowing edge

and the linear map $L_{\gamma,\gamma'} = L^{\chi}_{\gamma,\gamma'} : \Pi_{\gamma,\gamma'} \to \Pi_{\gamma'}$

$$L_{\gamma,\gamma'}(y) := \left(y_\sigma - \frac{\chi^v_\sigma}{\chi^v_{\sigma_*}} y_{\sigma_*} \right)_{\sigma \in F}. \tag{5.2}$$

Notice that $\Pi_{\gamma'} = \{ y \in \Pi_v : y_{\sigma_*} = 0 \}$

Proposition 5.4. *Given a vertex v of saddle type together with incoming and outgoing (flowing) edges γ, γ' as above, the sector $\Pi_{\gamma,\gamma'}$ is the set of points $y \in \mathrm{int}(\Pi_\gamma)$ which are connected by the orbit segment $\{ c(t) = y + t\chi^v : t \geq 0, c(t) \in \Pi_v \}$ to $L_{\gamma,\gamma'}(y) \in \mathrm{int}(\Pi_{\gamma'})$.*

Proof. Straightforward. □

The map $L_{\gamma,\gamma'}$ is a Poincaré for the flow of χ, which is represented by the following $F \times F$ matrix

$$M_{\gamma,\gamma'} = \left(\delta_{\sigma\sigma'} - \frac{\chi^v_\sigma}{\chi^v_{\sigma_*}} \delta_{\sigma_*\sigma'} \right)_{\sigma,\sigma' \in F}, \tag{5.3}$$

where δ stands for the Kronecker delta symbol. This matrix gives a global representation of the flow of χ which is suitable for computational purposes. The image of the map $L_{\gamma,\gamma'}$ is the convex cone $\Pi^{-\chi}_{\gamma',\gamma}$ associated with the vector field $-\chi$ and the pair γ', γ of reversed flowing edges. Clearly $L^{-\chi}_{\gamma',\gamma} = (L^{\chi}_{\gamma,\gamma'})^{-1}$.

Remark 5.5. *If v is a saddle type vertex then any line parallel to χ^v through a point in $\mathrm{int}(\Pi_v)$ must intersect at least two boundary facets of Π_v.*

Conversely, if an orbit segment $c(t) = p + t\,\chi^v$ through a point $p \in \mathrm{int}(\Pi_v)$ crosses the boundary of Π_v at two points, $q = p + t_0\,\chi^v$, with $t_0 < 0$, and $q' = p + t_1\,\chi^v$, with $t_1 > 0$, and if $\sigma', \sigma_* \in F_v$ are the facets of Π_v such that $q_{\sigma'} = 0$ and $q'_{\sigma_*} = 0$ then $\chi^v_{\sigma'} > 0$ and $\chi^v_{\sigma_*} < 0$. This implies that v is of saddle type.

In this setting, if γ, γ' are the edges through v, respectively in the corners (v, σ') and (v, σ_*), then $q \in \Pi_\gamma = \{ y \in \Pi_v : y_{\sigma'} = 0 \}$ and $q' \in \Pi_{\gamma'} = \{ y \in \Pi_v : y_{\sigma_*} = 0 \}$. Moreover, if both γ and γ' are flowing edges then $q \in \Pi_{\gamma,\gamma'}$ and $q' = L_{\gamma,\gamma'}(q)$.

If the vertex v is attractive or repelling (instead of saddle type), i.e., if all the characters χ_σ^v, with $\sigma \in F_v$, have the same sign, then $\Pi_{\gamma,\gamma'} = \emptyset$. In these cases, it is not possible to connect any point in Π_γ to a point of $\Pi_{\gamma'}$ through a line parallel to the constant vector χ^v, see Figure 11.

Remark 5.6. *Points in the boundary of Π_γ are in the intersection of three or more sectors Π_v with $v \in V$. Hence, if an orbit ends up in one of these points it is not possible to continue it in a unique way. In the sequel we disregard these types of orbits.*
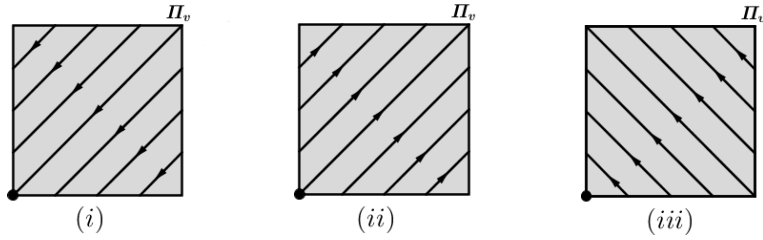

FIGURE 11. Vertex types: (i) attractive, (ii) repelling and (iii) saddle type

We now define *skeleton flow maps* along chains of saddle type vertexes. Let

$$v_0 \xrightarrow{\gamma_0} v_1 \xrightarrow{\gamma_1} v_2 \longrightarrow \ldots \longrightarrow v_m \xrightarrow{\gamma_m} v_{m+1} \tag{5.4}$$

be a chain of flowing-edges. The sequence $\xi = (\gamma_0, \gamma_1, \ldots, \gamma_m)$ will be called a *heteroclinic path*, a *heteroclinic cycle* when $\gamma_m = \gamma_0$.

Definition 5.7. Given a heteroclinic path $\xi = (\gamma_0, \gamma_1, \ldots, \gamma_m)$, we define the *skeleton flow map (of χ) along ξ* to be the composition mapping $\pi_\xi : \Pi_\xi \to \Pi_{\gamma_m}$

$$\pi_\xi := L_{\gamma_{m-1},\gamma_m} \circ \ldots \circ L_{\gamma_0,\gamma_1} ,$$

with domain

$$\Pi_\xi := \text{int}(\Pi_{\gamma_0}) \cap \bigcap_{j=1}^{m} (L_{\gamma_*,\gamma_j} \circ \ldots \circ L_{\gamma_0,\gamma_1})^{-1} \text{int}(\Pi_{\gamma_j}) .$$

For every $y \in \Pi_\xi$, $y \in \text{int}(\Pi_{\gamma_0})$, $\pi_\xi(y) \in \text{int}(\Pi_{\gamma_m})$ and moreover there exists an orbit segment from y to $\pi_\xi(y)$ with itinerary ξ.

We also define the matrix

$$M_\xi := M_{\gamma_{m-1},\gamma_m} \cdots M_{\gamma_1,\gamma_2} \, M_{\gamma_0,\gamma_1} \tag{5.5}$$

where the factor matrices $M_{\gamma_{j-1},\gamma_j}$ were defined in (5.3). This matrix M_ξ induces a linear endomorphism on $\mathbb{R}^F$ whose restriction to the sector Π_ξ matches the skeleton flow map π_ξ.

In order to analyze the dynamics of the flow of the skeleton vector field χ it is convenient to introduce the concept of *structural set* and its associated skeleton flow map.

Definition 5.8. A non-empty set of flowing edges S is said to be a *structural set* for χ if every heteroclinic cycle contains an edge in S.

Notice that the structural set S is in general not unique. The concept of structural set can be defined for general directed graphs. It corresponds to the homonym notion introduced by L. Bunimovich and B. Webb [4], but here applied to the line graph[4].

We say that a heteroclinic path $\xi = (\gamma_0, \ldots, \gamma_m)$ is a *branch* of S, or shortly an S-branch, if

    (1) $\gamma_0, \gamma_m \in S$,
    (2) $\gamma_j \notin S$ for all $j = 1, \ldots, m-1$.

We denote by $\mathscr{B}_S(\chi)$ the set of all S-branches.

Definition 5.9. The *skeleton flow map* $\pi_S : D_S \to \Pi_S$ is defined by

$$\pi_S(y) := \pi_\xi(y) \quad \text{for all } y \in \Pi_\xi,$$

where

$$\Pi_S := \cup_{\gamma \in S} \Pi_\gamma \quad \text{and} \quad D_S := \cup_{\xi \in \mathscr{B}_S(\chi)} \Pi_\xi.$$

We now provide a sufficient condition for the skeleton flow map π_S to be a closed dynamical system.

Proposition 5.10. *Given a skeleton vector field χ on $\mathcal{C}^*(\Gamma^d)$ and a structural set S, assume*

    (1) every edge of the polytope is either neutral or a flowing edge.
    (2) all vertexes are of saddle type,

Then D_S has full Lebesgue measure in Π_S.

Proof. The inclusion $D_S \subseteq \Pi_S$ is obvious.

For each flowing edge γ with $v = t(\gamma)$, let $D_\gamma := \cup_{s(\gamma')=v} \Pi_{\gamma,\gamma'}$, with the union taken over the set of flowing edges γ' such that $s(\gamma') = v$. Clearly $D_\gamma \subset \Pi_\gamma$. We claim that

$$\Pi_\gamma \setminus D_\gamma \subseteq \partial \Pi_\gamma \cup \bigcup_{\gamma' : s(\gamma')=t(\gamma)} L_{\gamma,\gamma'}^{-1}(\partial \Pi_{\gamma'})$$

which in particular implies that this set has codimension one in the sector Π_γ. Let us now prove the claim. By (2) the vertex v is of saddle type. Since $v = t(\gamma)$, the corner (v, γ) has positive character. Hence, given $q \in \text{int}(\Pi_\gamma)$ the orbit segment $c(t) := q + t\chi^v$ enters $\text{int}(\Pi_v)$ for t positive and small. By Remark 5.5, this orbit segment will eventually hit another boundary point $q' \in \Pi_{\gamma'} \subset \partial \Pi_v$ for some edge γ' through v. The same remark shows that χ has opposite signs at the corners (v, γ)

---

[4] The line graph of a directed graph G, denoted by $L(G)$, is the graph whose vertices are the edges of G, and where $(\gamma, \gamma') \in E \times E$ is an edge of $L(G)$ if the end-point of γ coincides with the start-point of γ'.

and (v, γ'). Thus, by item (1) γ' is also a flowing edge and $q' = L_{\gamma, \gamma'}(q)$. Therefore, if $q \notin D_\gamma$ then

$$q \in \bigcup_{\gamma' \, : \, s(\gamma') = v} L_{\gamma, \gamma'}^{-1}(\partial \Pi_{\gamma'})$$

which proves the claim.

Let $D = \cup_\gamma D_\gamma$ and $\Pi = \cup_\gamma \Pi_\gamma$ with the unions taken over all flowing edges. Define then a skeleton flow map $\pi \colon D \to \Pi$ setting $\pi(y) = L_{\gamma, \gamma'}(y)$ whenever γ, γ' are flowing edges such that $t(\gamma) = s(\gamma')$ and $y \in \Pi_{\gamma, \gamma'}$. The previous claim implies that D has ful Lebesgue measure in Π. In fact it shows that $\Pi \setminus D$ has codimension one in Π. The set $D_\infty = \cap_{n \geq 0} \pi^{-n}(D)$ has also full measure because $\pi : D \to \Pi$ is locally a linear isomorphism and $\Pi \setminus D_\infty = \cup_{n \geq 0} \pi^{-n}(\Pi \setminus D)$ is a countable union of sets with zero Lebesgue measure.

Consider now $y \in \Pi_S$, assume that $y \in D_\infty$ and consider the itinerary $(\gamma_0, \gamma_1, \dots)$ of the corresponding (forward) infinite orbit. Then $\gamma_0 \in S$. Assumptions (1)-(2) imply that the flowing edge graph has no terminal points. If we had $\gamma_j \notin S$ for all $j \geq 1$, there would be heteroclinic cycles disjoint from S, which contradicts the fact that S is a structural set. Hence some initial segment $\xi = (\gamma_0, \dots, \gamma_m)$ of this itinerary is an S-branch, and $y \in \Pi_\xi \subseteq D_S$. This proves that $\Pi_S \setminus D_S \subset \Pi \setminus D_\infty$ has zero Lebesgue measure. $\qquad \square$

Remark 5.11. *The proof of Proposition 5.10 shows that the maximal invariant set*

$$\hat{D}_S := \bigcap_{n \in \mathbb{Z}} (\pi_S)^{-n}(D_S)$$

has full Lebesgue measure in Π_S. Hence the skeleton flow map induces a homeomorphism $\pi_S : \hat{D}_S \to \hat{D}_S$ on the Baire space $\hat{D}_S$.

6. Asymptotic Poincaré Maps

In this section, we state and prove our main result. Given a structural set S consider the system of cross sections $\Sigma_S = \cup_{\gamma \in S} \Sigma_\gamma^-$ transversal to the flowing edges in S. Then the Poincaré map induced by the flow of a regular vector field $X \in \mathfrak{X}^\omega(\Gamma^d)$ on Σ_S is "asymptotically conjugate" to the skeleton flow map π_S of χ.

For any flowing edge γ through a vertex v define

$$\Sigma_{v, \gamma} := (\Psi_{v, \epsilon}^X)^{-1}(\mathrm{int}(\Pi_\gamma)).$$

This cross section is transversal to the flow of X and is an inner facet of the tubular neighborhood N_v. We will write Σ_γ^- or Σ_γ^+, instead of $\Sigma_{v, \gamma}$, according to the sign of the character χ at the corner (v, γ).

Let $\mathscr{D}_\gamma$ be the set of points $x \in \Sigma_\gamma^-$ such that the forward orbit of x has a transversal intersection with Σ_γ^+.

Definition 6.1. The global Poincaré map along γ, see Figure 1,

$$P_\gamma : \mathscr{D}_\gamma \subset \Sigma_\gamma^- \to \Sigma_\gamma^+$$

is defined by $P_\gamma(x) := \varphi_X^{\tau(x)}(x)$, where φ_X^t stands for the flow of X and

$$\tau(x) = \min\{\, t > 0 : \varphi_X^t(x) \in \Sigma_{v',\gamma} \,\} \, .$$

Both functions τ and P_γ are analytic.

Let

$$\Pi_\gamma(\epsilon) := \{\, y \in \Pi_\gamma : y_\sigma \geq \epsilon \quad \text{whenever} \quad \gamma \subset \sigma\}. \qquad (6.1)$$

Notice that $\lim_{\epsilon \to 0} \Pi_\gamma(\epsilon) = \text{int}(\Pi_\gamma)$. Given $k \in \mathbb{N}$ take $r = r(k, X)$ according to Lemma 4.7.

Lemma 6.2. *Given a flowing-edge*

$$(v, \sigma_0) \xrightarrow{\gamma} (v', \sigma'),$$

let $\mathscr{D}_\gamma^\epsilon \subset \Pi_\gamma(\epsilon^r)$ *be the domain of the map*

$$F_\gamma^\epsilon := \Psi_{v',\epsilon}^X \circ P_\gamma \circ (\Psi_{v,\epsilon}^X)^{-1}.$$

Then

$$\lim_{\epsilon \to 0^+} F_\gamma^\epsilon|_{\mathscr{D}_\gamma^\epsilon} = \text{id}_{\Pi_\gamma}$$

in the C^k topology, in the sense of Definition 4.6.

Proof. If $F_v = \{\sigma_0, \sigma_1, \sigma_2, \ldots, \sigma_{d-1}\}$ then $F_{v'} = \{\sigma_1, \ldots, \sigma_{d-1}, \sigma'\}$ and $\{\sigma \in F : \gamma \subset \sigma\} = \{\sigma_1, \ldots, \sigma_{d-1}\}$. Since inside Π_γ we have $y_\sigma = 0$ whenever $\gamma \not\subset \sigma$, we can express points in Π_γ as lists $(y_1, \ldots, y_{d-1})$ where each y_j abbreviates y_{σ_j}.

To simplify notations, let's use x_l and ν_l, respectively, for the coordinate and order associated to σ_l, where $l = 1, \ldots, d-1$. Consider the flow box $(V, (t, x_1, \ldots, x_{d-1}))$ with $V = N_\gamma$ and the coordinate system introduced in the beginning of Section 4. In this flow box the vector field's equation reads as:

$$\begin{cases} \dot{t} & = 1 \\ \dot{x}_l & = x_l^{\nu_l} H_l(t, x), \quad l = 1, \ldots, d-1, \end{cases} \qquad (6.2)$$

where $H_l(t, x)$ is defined in (3.1). Integrating

$$\frac{d}{dt} h_{\nu_l}(x_l) = -\dot{x}_l\, x_l^{-\nu_l} = -H_l(t, x) \quad l = 1, \ldots, d-1,$$

yields

$$h_{\nu_l}(x_l(t)) = h_{\nu_l}(x_l(0)) - \int_0^t H_l(\varphi^s(0, x(0)))\, ds \quad l = 1, \ldots, d-1,$$

where φ^t stands for the flow of the vector field (6.2). Therefore

$$P_\gamma(x) = \left\{ h_{\nu_l}^{-1}\left(h_{\nu_l}(x_l) - \int_0^{\tau(x)} H_l(\varphi^s(0, x))\, ds \right) \right\}_{l=1,\ldots,d-1} \qquad (6.3)$$

where $\tau(x)$ is the time that the orbit starting at $x \in \Sigma_\gamma^-$ takes to hit the cross-section Σ_γ^+.

Expressing $(\Psi_{v,\epsilon}^X)^{-1}$ in the coordinate system $(x_0, x_1, \ldots, x_{d-1})$ on the neighborhood N_v, for every point $(y_1, \ldots, y_{d-1}) \in \Pi_\gamma$,

$$(\Psi_{v,\epsilon}^X)^{-1}(y) = \left(1, h_{\nu_1}^{-1}(\frac{y_1}{\epsilon^2}), \ldots, h_{\nu_{d-1}}^{-1}(\frac{y_{d-1}}{\epsilon^2})\right).$$

By (6.3) we have

$$P_\gamma\left(\Psi_{v,\epsilon}^{-1}(y)\right) = \left(h_{\nu_l}^{-1}\left[h_{\nu_l}(h_{\nu_l}^{-1}(\frac{y_l}{\epsilon^2})) - \int_0^{\tau(\Psi_{v,\epsilon}^{-1}(y))} H_l\, ds\right]\right)_{1 \le l \le d-1}.$$

Hence $F_\gamma^\epsilon(y_1, \ldots, y_{d-1}) = (y_1'(\epsilon), \ldots, y_{d-1}'(\epsilon))$, where by Definition 4.3

$$y_l'(\epsilon) = \epsilon^2 h_{\nu_l}\left(h_{\nu_l}^{-1}\left[h_{\nu_l}(h_{\nu_l}^{-1}(\frac{y_l}{\epsilon^2})) - \int_0^{\tau(\Psi_{v,\epsilon}^{-1}(y))} H_l\, ds\right]\right)$$

$$= y_l - \epsilon^2 \int_0^{\tau((\Psi_{v,\epsilon})^{-1}(y))} H_l(\varphi^s(\Psi_{v,\epsilon}^{-1}(y)))\, ds.$$

Notice that τ is analytic, and together with its derivatives is locally bounded in a neighborhood of $\gamma \cap \Sigma_\gamma^-$. Moreover, every derivative $(D^k\varphi^t)_x$ is a solution of a system of linear equations with coefficients depending on $\varphi^t(x)$ and on the lower order derivatives $(D^r\varphi^t)_x$ with $r < k$. Arguing recursively, we can prove that for any $k \ge 0$ the k-th order derivatives of $H_l(t, \varphi^t(x))$ are uniformly bounded in a neighborhood of $\gamma \cap \Sigma_\gamma^-$, for $0 \le t \le \tau(x)$. Hence, it follows from item (1) of Lemma 4.5 that F_ϵ converges to the identity map in the C^k topology. $\square$

Remark 6.3. *By Lemma 6.2, for any flowing edge $v \xrightarrow{\gamma} v'$, we can identify the two sections Σ_γ^- and Σ_γ^+. We will refer to the identified section simply as Σ_γ.*

Let γ, γ' be flowing edges such that $t(\gamma) = s(\gamma') = v$. We denote by $\mathscr{D}_{\gamma,\gamma'}$ the set of points $x \in \Sigma_{v,\gamma}$ such that the forward orbit of x has a transversal intersection with $\Sigma_{v,\gamma'}$.

Definition 6.4. The local Poincaré map

$$P_{\gamma,\gamma'} : \mathscr{D}_{\gamma,\gamma'} \subset \Sigma_{v,\gamma} \to \Sigma_{v,\gamma'}$$

is defined by $P_{\gamma,\gamma'}(x) := \varphi_X^{\tau(x)}(x)$, see Figure 1, where

$$\tau(x) = \min\{\, t > 0 : \varphi_X^t(x) \in \Sigma_{v,\gamma'}\,\}.$$

Given $k \in \mathbb{N}$ take $r = r(k, X)$ according to Lemma 4.7.

Lemma 6.5. *Given flowing edges γ, γ' such that $t(\gamma) = s(\gamma') = v$, let $\mathscr{D}_{\gamma,\gamma'}^\epsilon \subset \Pi_\gamma(\epsilon^r)$ be the domain of the map*

$$F_{\gamma,\gamma'}^\epsilon := \Psi_{v,\epsilon}^X \circ P_{\gamma,\gamma'} \circ (\Psi_{v,\epsilon}^X)^{-1}.$$

Then

$$\lim_{\epsilon \to 0^+} \left(F^\epsilon_{\gamma,\gamma'} \right)_{|\mathscr{D}^\epsilon_{\gamma,\gamma'}} = L_{\gamma,\gamma'}$$

in the C^k topology, in the sense of Definition 4.6.

Proof. Setting $F_v = \{\sigma_0, \sigma_1, \ldots, \sigma_{d-1}\}$ consider the system of coordinates $(y_0, y_1, \ldots, y_{d-1})$ on Π_v where each y_j abbreviates y_{σ_j}. Assume the facets in F_v were ordered in a way that

$$\Pi_\gamma = \{y \in \Pi_v : y_0 = 0\} \quad \text{and} \quad \Pi_{\gamma'} = \{y \in \Pi_v : y_{d-1} = 0\}.$$

Let

$$\partial_\gamma \Pi_v(\epsilon^r) := \{y \in \Pi_v(\epsilon^r) : y_0 = \epsilon^r\}$$
$$\partial_{\gamma'} \Pi_v(\epsilon^r) := \{y \in \Pi_v(\epsilon^r) : y_{d-1} = \epsilon^r\}$$

be the boundary facets of the sector $\Pi_v(\epsilon^r)$ defined in (4.4), respectively, parallel to Π_γ and $\Pi_{\gamma'}$. By Lemma 4.7, the Poincaré map of the vector field $(\Psi^X_{v,\epsilon})_* X = \epsilon^2 \tilde{X}^\epsilon_v$ from $\partial_\gamma \Pi_v(\epsilon^r)$ to $\partial_{\gamma'} \Pi_v(\epsilon^r)$ converges in the C^k topology to $(L_{\gamma,\gamma'})_{|\Pi_{\gamma,\gamma'}}$. We are left to prove that, see Figure 12, the Poincaré maps of this vector field from

$$\Pi_\gamma(\epsilon^r) = \{y \in \Pi_v : y_0 = 0 \text{ and } y_1, \ldots, y_{d-1} \le \epsilon^r\}$$

to $\partial_\gamma \Pi_v(\epsilon^r)$, and from $\partial_{\gamma'} \Pi_v(\epsilon^r)$ to

$$\Pi_{\gamma'}(\epsilon^r) = \{y \in \Pi_v : y_{d-1} = 0 \text{ and } y_0, \ldots, y_{d-2} \le \epsilon^r\}$$

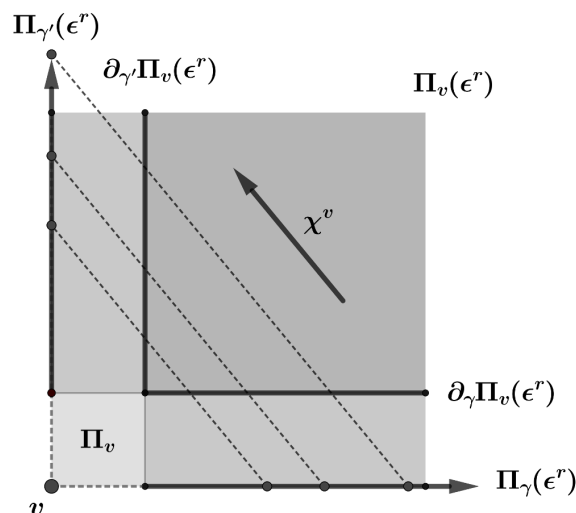converge to the identity maps in the C^k topology as $\epsilon \to 0^+$.

FIGURE 12. The local map $L_{\gamma,\gamma'}$ factors as a composition of three projections.

The two convergences are analogous and we only prove the first one. The argument is similar to that of Lemma 6.2, but instead of (6.2) we consider the equations of X

$$\dot{x}_l = x_l^{\nu_l} H_l(x) \quad 0 \le l \le d - 1 \tag{6.4}$$

represented in the system of coordinates $(x_0, x_1, \ldots, x_{d-1})$ on N_v.

Notice that $(\Psi_{v,\epsilon}^X)^{-1} \Pi_\gamma(\epsilon^r) \subset \Sigma_{v,\gamma}$ is defined by the conditions

$$x_0 = 1 \ \text{ and } \ 0 < x_l < h_{\nu_l}^{-1}\left(\frac{1}{\epsilon^{2-r}}\right), \quad 1 \le l \le d - 1.$$

Likewise, $\Sigma_{v,\gamma}^\epsilon := (\Psi_{v,\epsilon}^X)^{-1} \partial_\gamma \Pi_v(\epsilon^r)$ is defined by $x_0 = h_{\nu_0}^{-1}(\frac{1}{\epsilon^{2-r}})$ and the same conditions above in the remaining coordinates. Let $\tau^\epsilon(x)$ denote the time that the orbit starting at $x \in \Sigma_{v,\gamma}$ takes to hit the cross-section $\Sigma_{v,\gamma}^\epsilon$. Integrating the first component of (6.4), we have

$$h_{\nu_0}\left(h_{\nu_0}^{-1}\left(\frac{1}{\epsilon^{2-r}}\right)\right) - h_{\nu_0}(1) = -\int_0^{\tau^\epsilon(x)} H_0(\varphi^s(x)) ds. \tag{6.5}$$

Since $-H_0(v) = \chi_{\sigma_0}^v > 0$ there exists a neighborhood U_v of v where $-H_0$ takes positive values. We can take a constant $C > 0$ and shrink U_v so that $-H_0 \ge \frac{1}{C}$ and $\|D^r H_0\| \le C$ for all $1 \le r \le k$ on U_v. Without loss of generality we may assume that $\Sigma_{v,\gamma}$ is contained in U_v. From (6.5) we have

$$\int_0^{\tau^\epsilon(x)} -H_0(\varphi^s(x)) \, ds = \frac{1}{\epsilon^{2-r}}, \tag{6.6}$$

which implies

$$\tau^\epsilon(x) \le \frac{C}{\epsilon^{2-r}}.$$

Differentiating both sides of (6.6) with respect to x_l, for $1 \le l \le d - 1$, we obtain

$$H_0(\varphi^{\tau^\epsilon(x)}(x)) \frac{\partial \tau^\epsilon(x)}{\partial x_l} + \int_0^{\tau^\epsilon(x)} \nabla H_0(\varphi^s(x)) \cdot \frac{\partial \varphi^s(x)}{\partial x_l} \, ds = 0. \tag{6.7}$$

Similar formulas can be driven for higher order derivatives of τ^ϵ.

Arguing as in Lemma 6.2, we can bound the derivatives of the flow $\varphi^s(x)$. Since the derivatives of H_0 are also bounded, we infer from (6.7), and its higher order analogues, that the function τ^ϵ has bounded derivatives up to order k. Finally, repeating the argument in the proof of Lemma 6.2, we conclude that the Poincaré map from $\Pi_\gamma(\epsilon^r)$ to $\partial_\gamma \Pi_v(\epsilon^r)$ converges to identity in the C^k topology as $\epsilon \to 0^+$. $\square$

Definition 6.6. Given a heteroclinic path $\xi = (\gamma_0, \gamma_1, \ldots, \gamma_m)$, the composition

$$P_\xi := (P_{\gamma_m} \circ P_{\gamma_{m-1}, \gamma_m}) \circ \ldots \circ (P_{\gamma_1} \circ P_{\gamma_0, \gamma_1})$$

is referred to as the *Poincaré map* of the vector field X along ξ. The domain of this composition is denoted by $\mathscr{D}_\xi$.

Lemmas 6.2 and Lemma 6.5 imply that given a heteroclinic path ξ, the asymptotic behavior of the Poincaré map P_ξ along ξ is given by the corresponding Poincaré map π_ξ of the skeleton vector field χ. More precisely, given $k \in \mathbb{N}$ and taking $r = r(k, X)$ according to Lemma 4.7 we have

Proposition 6.7. *Given a heteroclinic path $\xi = (\gamma_0, \dots, \gamma_m)$ with $v_0 = s(\gamma_0)$ and $v_m = s(\gamma_m)$, let $\mathscr{D}_\xi^\epsilon$ be the domain of the composite map $F_\xi^\epsilon := \Psi_{v_m,\epsilon}^X \circ P_\xi \circ (\Psi_{v_0,\epsilon}^X)^{-1}$ from $\Pi_{\gamma_0}(\epsilon^r)$ into $\Pi_{\gamma_m}(\epsilon^r)$. Then*

$$\lim_{\epsilon \to 0^+} \left(F_\xi^\epsilon \right)_{|\mathscr{D}_\xi^\epsilon} = \pi_\xi$$

in the C^k topology, in the sense of Definition 4.6.

Proof. Follows immediately from Lemmas 6.2 and 6.5. $\square$

As mentioned in the introduction, we are interested in studying the flow of X along heteroclinic cycles on the polytope's vertex-edge network. To encode the semi-global dynamics of the flow φ_X^t along the cycles, we use Poincaré return maps to a system of cross-sections Σ_γ, see Remark 6.3, placed at the edges of a structural set, see Definition 5.8. Any orbit of the flow φ_X^t that shadows some heteroclinic cycle must intersect these cross-sections in a recurrent way.

Definition 6.8. Let $X \in \mathfrak{X}^\omega(\Gamma^d)$ be a vector field with a structural set $S \subset E$. We define the S-Poincaré map $P_S : \mathscr{D}_S \subset \Sigma_S \to \Sigma_S$ setting $\Sigma_S := \cup_{\gamma \in S} \Sigma_\gamma$, $\mathscr{D}_S := \cup_{\xi \in \mathscr{B}_S(\chi)} \mathscr{D}_\xi$ and $P_S(p) := P_\xi(p)$ for all $p \in \mathscr{D}_\xi$. Note that the domains $\mathscr{D}_\xi$ and $\mathscr{D}_{\xi'}$ are disjoint for $\xi \neq \xi'$ in $\mathscr{B}_S(\chi)$.

By construction the suspension of the S-Poincaré map $P_S : D_S \subset \Sigma_S \to \Sigma_S$ embeds (up to a time re-parametrization) in the flow of the vector field X. In this sense the dynamics of the map P_S encapsulates the qualitative behavior of the flow φ_X^t of X along the edges of Γ^d.

Theorem 6.9. *Let $X \in \mathfrak{X}^\omega(\Gamma^d)$ be a regular vector field with skeleton vector field χ and a structural set $S \subset E_\chi$. Then*

$$\lim_{\epsilon \to 0^+} \Psi_\epsilon \circ P_S \circ (\Psi_\epsilon)^{-1} = \pi_S$$

in the C^∞ topology, in the sense of Definition 4.6.

Proof. Follows from Proposition 6.7. $\square$

7. Asymptotic integrals of motion

In this section we introduce a probe space $\mathcal{H}(\Gamma^d)$ for integrals of motion of the vector fields in $\mathfrak{X}^\omega(\Gamma^d)$. This space consists of analytic functions in $\mathrm{int}(\Gamma^d)$ with poles at the polytope's facets. We show that a function $h \in \mathcal{H}(\Gamma^d)$ rescales to a piecewise linear function $\eta : \mathcal{C}^*(\Gamma^d) \to \mathbb{R}$ on the dual cone. Moreover, if $h \in \mathcal{H}(\Gamma^d)$ is an integral of motion of

a vector field $X \in \mathfrak{X}^\omega(\Gamma^d)$ then η is also an integral of motion for the piecewise linear flow of the skeleton vector field χ of X.

Recalling that $\{f_\sigma\}_{\sigma \in F}$ is a defining family of the polytope Γ^d, let $\mathcal{F} = \{h_n \circ f_\sigma, : \ n \geq 1, \sigma \in F\}$ where h_n was introduced in (4.2), and define $\mathcal{H}(\Gamma^d)$ to be the linear span of $\mathcal{C}^\omega(\Gamma^d) \cup \mathcal{F}$. Since functions in the set $\mathcal{F}$ are linearly independent and $\mathcal{H}(\Gamma^d) = \mathcal{C}^\omega(\Gamma^d) \oplus \langle \mathcal{F} \rangle$, each $h \in \mathcal{H}$ can be uniquely decomposed as

$$h = g + \sum_{n=1}^{\infty} \sum_{\sigma \in F} \mu_{n\sigma} \left(h_n \circ f_\sigma \right), \qquad (7.1)$$

with $g \in \mathcal{C}^\omega(\Gamma^d)$, where only a finite number of coefficients $\mu_{n\sigma}$ are nonzero. Note that the differential dh is given by the expression:

$$dh = dg \ - \ \sum_{n=1}^{\infty} \sum_{\sigma \in F} \mu_{n\sigma} \frac{df_\sigma}{(f_\sigma)^n} \ . \qquad (7.2)$$

We define the *order of h at* σ to be the number

$$\nu^h(\sigma) = \max\{n \in \mathbb{N} \colon \mu_{n\sigma} \neq 0\},$$

with $\nu^h(\sigma) = 0$ if all $\mu_{n\sigma} = 0$. The map $\nu^h : F \to \mathbb{N}$ is referred to as the *order function* of h.

Definition 7.1. The character of h at σ is the coefficient $\eta^h(\sigma) = \mu_{n\sigma}$ corresponding to the term with largest order $n = \nu^h(\sigma)$. The character is undefined if $\nu^h(\sigma) = 0$. We say that the function

$$\eta^h : \mathcal{C}^*(\Gamma^d) \to \mathbb{R} , \quad \eta^h(y) := \sum_{\sigma \in F} \eta^h(\sigma) \, y_\sigma$$

is the skeleton of h.

Proposition 7.2. *Given a regular vector field $X \in \mathfrak{X}^\omega(\Gamma^d)$ and a function $h \in \mathcal{H}(\Gamma^d)$ with the same order function $\nu : F \to \mathbb{N}$, let χ be the skeleton of X and $\eta : \mathcal{C}^*(\Gamma^d) \to \mathbb{R}$ be the skeleton of h. Then*

  (1) $\eta = \lim_{\epsilon \to 0^+} \epsilon^2 h \circ (\Psi^X_{v,\epsilon})^{-1}$ over $\mathrm{int}(\Pi_v)$ for any vertex v, with convergence in the C^∞ topology.
  (2) $d\eta = \lim_{\epsilon \to 0^+} \epsilon^2 \left[(\Psi^X_{v,\epsilon})^{-1} \right]^* (dh)$ over $\mathrm{int}(\Pi_v)$ for any vertex v, with convergence in the C^∞ topology.
  (3) If h is invariant under the flow of X, i.e., $dh(X) \equiv 0$, then η is invariant under the skeleton flow of χ, i.e., $d\eta(\chi) \equiv 0$.

Remark 7.3. *Since ν is the order function of X, $\nu(\sigma) \geq 1$ for every facet $\sigma \in F$. Hence, because ν is also the order function of h the skeleton character $\eta(\sigma) = \eta^h(\sigma)$ is well defined for all facets $\sigma \in F$.*

Proof. Consider the system of local coordinates $x = (x_\sigma)_{\sigma \in F_v} = (f_\sigma(q))_{\sigma \in F_v}$ on the neighborhood N_v. According to decomposition (7.1) we can

write

$$h(x) = g(x) + \sum_{\sigma \in F_v} \sum_{n=1}^{\nu(\sigma)} \mu_{n\sigma} \, h_n(x_\sigma) \, ,$$

where $g(x)$ is analytic in N_v. Therefore, by item (2) of Lemma 4.5,

$$\epsilon^2 \, h \circ (\Psi^X_\epsilon)^{-1}(y) = \epsilon^2 \, g \circ (\Psi^X_\epsilon)^{-1}(y) + \epsilon^2 \sum_{\sigma \in F_v} \sum_{n=1}^{\nu(\sigma)} \mu_{n\sigma} \left(h_n \circ h^{-1}_{\nu(\sigma)} \right) \left(\frac{y_\sigma}{\epsilon^2} \right)$$

converges in the C^∞ topology to $\sum_{\sigma \in F_v} \mu_{\nu(\sigma)\sigma} \, y_\sigma = \eta(y)$ over the sector $\mathrm{int}(\Pi_v)$. This proves (1) and also implies (2).

For item (3) we use the following abstract result. Given a smooth function h and a smooth vector field X on a manifold M, and given a diffeomorphism $\Psi : M \to N$,

$$dh(X) \circ \Psi^{-1} = d(h \circ \Psi^{-1})[\Psi_* X].$$

Since we are assuming that $dh(X) \equiv 0$, by item (2) and Lemma 4.7

$$\begin{aligned}
0 = dh(X) \circ \Psi^X_{v,\epsilon} &= d(h \circ (\Psi^X_{v,\epsilon})^{-1})[(\Psi^X_{v,\epsilon})_* X] \\
&= d(\epsilon^2 h \circ (\Psi^X_{v,\epsilon})^{-1})[\epsilon^{-2}(\Psi^X_{v,\epsilon})_* X] \\
&= d(\epsilon^2 h \circ (\Psi^X_{v,\epsilon})^{-1})[\, \tilde{X}^\epsilon_v] \longrightarrow d\eta(\chi^v)
\end{aligned}$$

as $\epsilon \to 0$. This proves that the piecewise linear function η is invariant under the flow of the skeleton vector field χ. $\qquad\square$

A continuous function $h : M \to \mathbb{R}$ is said to be *proper* if for all real numbers $a < b$ the pre-image $f^{-1}[a,b] \subset M$ is compact.

Proposition 7.4. *If $h \in \mathcal{H}(\Gamma^d)$ is proper in $\mathrm{int}(\Gamma^d)$ with order function $\nu \geq 1$ then its skeleton $\eta : \mathcal{C}^*(\Gamma^d) \to \mathbb{R}$ is also a proper function.*

Proof. Fix a vertex v and let $F_v = \{\sigma_1, \ldots, \sigma_d\}$. Take the usual system of affine coordinates $(x_1, \ldots, x_d)$ on the neighborhood N_v where $x_j = f_{\sigma_j}$. In these coordinates h can be written as

$$h(x) = g(x) + \sum_{j=1}^d \frac{p_j(x)}{x^{\nu_j}}$$

where $g(x)$ is analytic in N_v, ν_j is the order of h at σ_j and each $p_j(x)$ is a polynomial function such that $\mu_j = p_j(0) \neq 0$ is the character of h at σ_j. On the sector Π_v the skeleton η of h is given by $\eta(y_1, \ldots, y_d) = \sum_{j=1}^d \mu_j y_j$. Since h is proper, the level set $h^{-1}(0)$ is compact, which implies that h does not change sign in a small neighborhood of v. Hence we can assume that $h > 0$ on N_v. Because $h(x)$ is equal to $\sum_{j=1}^d \frac{\mu_j}{x^{\nu_j}}$ pus higher order terms as $x \to v$, all coefficients μ_j must be positive. Therefore

$$\eta^{-1}([a,b]) \cap \Pi_v \subset \{(y_1, \ldots, y_d) : y_j \geq 0, \ \sum_{j=1}^d \mu_j y_j \leq b\}$$

is a compact set. Because v is arbitrary, $\eta^{-1}([a,b])$ is also compact. $\qquad\square$

Remark 7.5. *Polymatrix replicator systems form a large class of models in EGT, that includes replicator and bimatrix replicator systems, falling within the scope of this work. The phase space of polymatrix replicators are prisms (products of simplexes), basic examples of simple polytopes. In [1] the first two authors have characterized the class of Hamiltonian polymatrix replicator systems w.r.t. a class of algebraic Poisson structures. All these models illustrate the conclusions of propositions 7.2 and 7.4.*

Remark 7.6. *If X is a Hamiltonian polymatrix replicator vector field w.r.t. some algebraic Poisson structure in the interior of a prism Γ^d, which has a proper Hamiltonian function h, then its skeleton flow map is volume preserving on each level set of the skeleton of h. This fact will not be proved here, see more in Section 10.*

Throughout the rest of this section we assume:
  (1) $X \in \mathfrak{X}^\omega(\Gamma^d)$ is a regular vector field, with skeleton χ, such that all vertexes are of saddle type and every edge is either neutral or a flowing edge;
  (2) X has integrals of motion $h_1, \ldots, h_k \in \mathcal{H}(\Gamma^d)$, all with the same order function as X;
  (3) $\eta_1, \ldots, \eta_k : \mathcal{C}^*(\Gamma^d) \to \mathbb{R}$ are respectively the skeletons of $h_1, \ldots, h_k$ and the forms $d\eta_1, \ldots, d\eta_k$ are linearly independent on every sector Π_v.

Consider the function $\eta : \mathcal{C}^*(\Gamma^d) \to \mathbb{R}^k$ defined by

$$\eta(y) := (\eta_1(y), \ldots, \eta_k(y)) .$$

Given a structural set S of χ and $c \in \mathbb{R}^k$ we define

$$\Delta_{S,c} := \Pi_S \cap \eta^{-1}(c). \qquad (7.3)$$

Given an edge γ or a branch $\xi \in \mathscr{B}_S(\chi)$ we also define

$$\Delta_{\gamma,c} := \Pi_\gamma \cap \eta^{-1}(c), \quad \Delta_{\xi,c} := \Pi_\xi \cap \eta^{-1}(c). \qquad (7.4)$$

Notice that

$$\Delta_{S,c} = \bigcup_{\xi \in \mathscr{B}_S(\chi)} \Delta_{\xi,c}. \qquad (7.5)$$

Theorem 7.7. *Under assumptions (1)-(3), given a structural set S of χ, the skeleton flow map $\pi_S : D_S \to \Pi_S$ induces a closed dynamical system on every level set $\Delta_{S,c}$ with $c = (c_1, \ldots, c_k) \in \mathbb{R}^k$.*

Proof. Follows from propositions 5.10 and 7.2. $\qquad\square$

Theorem 7.8. *Under assumptions (1)-(3), given a structural set S of χ, if $p \in \Delta_{S,c}$ is a hyperbolic periodic point of $\pi_{S|\Delta_{S,c}}$, and q is an associated transversal homoclinic point whose orbit has a compact*

closure contained in $\Delta_{S,c}$, then there exists a (compact) hyperbolic basic set contained in $\Delta_{S,c}$ for the map $\pi_{S|\Delta_{S,c}}$. Moreover each level set

$$L_\epsilon := \Gamma^d \cap \bigcap_{j=1}^{k} \left\{ h_j = \frac{c_j}{\epsilon^2} \right\},$$

with ϵ sufficiently small, contains a hyperbolic basic set for the S-Poincaré map $P_{S|L_\epsilon \cap \mathscr{D}_S}$, conjugated to the previous one.

Proof. Given $p \in \Delta_{S,c}$ and its associated transversal homoclinic point q consider an open neighborhood U of the π_S-orbits of p and q whose closure satisfies

$$\overline{U} \subset D_S = \bigcup_{\xi \in \mathscr{B}_S(\chi)} \Pi_\xi.$$

Because $\Lambda_0 := \{\pi_S^j(p) : j \in \mathbb{Z}\} \cup \{\pi_S^j(q) : j \in \mathbb{Z}\} \subset U$ is a hyperbolic set, reducing the size of U, the maximal invariant set $\Lambda = \cap_{j \in \mathbb{Z}} \pi_S^{-j}(\overline{U})$ is a hyperbolic basic set for $\pi_{S|\Delta_{S,c}}$.

Consider now the system of cross-sections $\Sigma_S := \cup_{\gamma \in S} \Sigma_\gamma^-$ transversal to the flow of X and let P_S denote the induced Poincaré map on Σ_S. By Theorem 6.9, the conjugated Poincaré map $\tilde{P}_S^\epsilon := \Psi_\epsilon \circ P_S \circ (\Psi_\epsilon)^{-1}$ on the (invariant) level set

$$\Pi_S \cap \Psi_\epsilon^X(L_\epsilon) = \Pi_S \cap \bigcap_{j=1}^{k} \left\{ \epsilon^2 h_j \circ (\Psi_\epsilon^X)^{-1} = c_j \right\}$$

can be seen as a small perturbation of the skeleton flow map $\pi_{S|\Delta_{S,c}}$. Notice that, according to Proposition 7.2 the level set $\Pi_S \cap \Psi_\epsilon^X(L_\epsilon)$ converges to $\Delta_{S,c}$ as $\epsilon \to 0$. Thus, because hyperbolic basic sets are structurally stable, see[19, Theorem 8.3], there exists a hyperbolic basic set $\tilde{\Lambda}_\epsilon$ for the conjugated Poincaré map $\tilde{P}_S^\epsilon$ on $\Pi_S \cap \Psi_\epsilon^X(L_\epsilon)$. Finally by conjugacy $\Lambda_\epsilon := (\Psi_\epsilon^X)^{-1}(\tilde{\Lambda}_\epsilon) \subset L_\epsilon$ is a hyperbolic basic set for the Poincaré map $P_{S|\Sigma_S \cap L_\epsilon}$ of the flow of X. $\qquad\square$

8. Procedure to analyze the dynamics

In this section we briefly describe the computational steps that through Theorem 7.8 lead to the detection of hyperbolic basic sets.

Input data: The polytope Γ^d and the vector field $X \in \mathfrak{X}^\omega(\Gamma^d)$.

Step 1. *Compute the character χ of X and draw its flowing-edge graph.* This step involves computing some derivatives at the vertex singularities. It can be done through a computer algebra system algorithm.

Step 2. *Find a structural set S for χ.* The search can be done by inspection if the flowing-edge graph is simple, or else using an algorithm for that purpose.

Step 3. *Determine all S-branches of χ.* Once the structural set is known, a simple algorithm determines its branches.

Step 4. *Find the integrals of motion of X in $\mathcal{H}(\Gamma^d)$ and determine their skeletons.* For instance if X is Hamiltonian with respect to some Poisson structure, join to the Hamiltonian function of X all the Casimirs of its Poisson structure.

Step 5. *Make explicit the skeleton flow map $\pi_S : \Pi_S \to \Pi_S$.* Use an algorithm to compute for each branch $\xi \in \mathscr{B}(\chi)$ the matrix M_ξ as well as the inequalities defining the domain Π_ξ. Then represent (computationally) the flow map π_S as a function defined by cases.

Step 6. *Compute some random orbits of π_S and determine their itineraries,* using the previous step representation of the flow map π_S.

Step 7. *Pick a few heteroclinic cycles ξ from the previous itineraries and compute the eigenvalues and eigenvectors of M_ξ.* Use an algorithm to compute a matrix's eigenvalues and eigenvectors. Every matrix M_ξ is a projection of $\mathbb{R}^F$ onto a $(d-1)$-dimensional subspace and hence has exactly $|F| - d + 1$ zero eigenvalues. If k integrals of motion were found in Step 4, the eigenspace of M_ξ associated with eigenvalue 1, $\mathrm{Ker}(M_\xi - I)$, must have at least dimension k.

Step 8. *Among the positive eigenvectors associated with eigenvalue 1 of M_ξ look for saddle type periodic points $p = \pi_S^n(p)$.* Any eigenvector $y \in \mathrm{Ker}(M_\xi - I)$ with non-negative entries belongs to the dual cone and is a prospective periodic point of π_S, but one still needs to verify that $y \in \Pi_\xi$.

Step 9. *Fix the level c such that $p \in \Delta_{S,c}$.*

Step 10. *Compute the local stable and unstable manifolds of p inside the component $\Delta_{\xi,c} \subseteq \Delta_{S,c}$ that contains p.*

Step 11. *Iterate the local stable manifold backward and the local unstable manifold forward, looking for transversal intersections.*

9. Examples

We will now present two examples, both replicators, illustrating the procedure detailed in the previous section. The second example belongs to a class of systems studied by Wang *et al.* [21].

By Theorem 7.8 the dynamics of these two systems are chaotic, *i.e.*, their flows contain horse-shoes, in sufficiently large levels.

9.1. **Example 1.** Consider the replicator system defined by matrix

$$A = \begin{pmatrix} 0 & -2 & 2 & 0 & 0 & 3 \\ 2 & 0 & -2 & 0 & 0 & 0 \\ -2 & 2 & 0 & -2 & 2 & 0 \\ 0 & 0 & 2 & 0 & -2 & 0 \\ 0 & 0 & -2 & 2 & 0 & -3 \\ -3 & 0 & 0 & 0 & 3 & 0 \end{pmatrix}.$$

We denote by X_A the vector field associated to this replicator defined on the simplex Δ^5. The point

$$q = \left(\frac{72}{245}, \frac{33}{280}, \frac{72}{245}, \frac{33}{280}, \frac{72}{245}, -\frac{23}{196} \right) \in \mathbb{R}^6$$

satisfies

(1) $(Aq)_1 = (Aq)_2 = (Aq)_3 = (Aq)_4 = (Aq)_5 = 0$;
(2) $q_1 + q_2 + q_3 + q_4 + q_5 = 1$,

and hence is an equilibrium of X_A, see [2, Definition 4.1]. Since matrix A is skew-symmetric, the associated replicator is conservative, *i.e.*, X_A is Hamiltonian with respect to some stratified Poisson structure on Δ^5, see [2, Definition 4.3, Proposition 12].

The polytope Δ^5 has five faces labeled by an index j ranging from 1 to 6, and designated by $\sigma_1, \ldots, \sigma_6$. The vertexes of the phase space Δ^5 are also labeled by $i \in \{1, \ldots, 6\}$, where the label i stands for the point $e_i \in \Delta^5$. To simplify the notation we designate the simplex's vertexes by $v_1, \ldots, v_6$. The skeleton character χ_A of X_A is displayed in Table 1.

χ_σ^v	σ_1	σ_2	σ_3	σ_4	σ_5	σ_6
v_1	0	-2	2	0	0	3
v_2	2	0	-2	0	0	0
v_3	-2	2	0	-2	2	0
v_4	0	0	2	0	-2	0
v_5	0	0	-2	2	0	-3
v_6	-3	0	0	0	3	0

TABLE 1. The skeleton character χ_A of X_A.

The edges of Δ^5 are designated by $\gamma_1, \ldots, \gamma_{15}$, according to Table 2, where we write $\gamma = (i\,j)$ to mean that γ is an edge connecting the vertexes v_i and v_j. This model has 15 edges: 7 neutral edges, $\gamma_3, \gamma_4, \gamma_7, \gamma_8, \gamma_9, \gamma_{12}, \gamma_{14}$, and 8 flowing-edges, $\gamma_1, \gamma_2, \gamma_5\gamma_6, \gamma_{10}, \gamma_{11}, \gamma_{13}, \gamma_{15}$. The flowing-edge directed graph of χ_A is depicted in Figure 13.
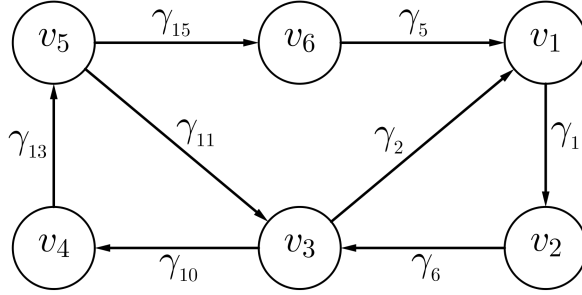
From this graph we can see that

$$S = \{ \gamma_6 = (2\,3), \gamma_{10} = (3\,4) \}$$

$\gamma_1 = (1\,2)$	$\gamma_2 = (1\,3)$	$\gamma_3 = (1\,4)$	$\gamma_4 = (1\,5)$	$\gamma_5 = (1\,6)$
$\gamma_6 = (2\,3)$	$\gamma_7 = (2\,4)$	$\gamma_8 = (2\,5)$	$\gamma_9 = (2\,6)$	$\gamma_{10} = (3\,4)$
$\gamma_{11} = (3\,5)$	$\gamma_{12} = (3\,6)$	$\gamma_{13} = (4\,5)$	$\gamma_{14} = (4\,6)$	$\gamma_{15} = (5\,6)$

TABLE 2. Edge labels.

is a structural set for χ_A, see Definition 5.8, whose S-branches denoted by $\xi_1, \ldots, \xi_5$ are displayed in Table 3, where we write $\xi_i = (j\,k\,l\,\ldots)$ to mean that ξ_i is a path from vertex v_j passing along vertices $v_k, v_l, \ldots$.

FIGURE 13. The oriented graph of χ_A.

From\To	$\gamma_6 = (2\,3)$	$\gamma_{10} = (3\,4)$
$\gamma_6 = (2\,3)$	$\xi_1 = (2\,3\,1\,2\,3)$	$\xi_2 = (2\,3\,4)$
$\gamma_{10} = (3\,4)$	$\xi_3 = (3\,4\,5\,3\,1\,2\,3)$ $\xi_4 = (3\,4\,5\,6\,1\,2\,3)$	$\xi_5 = (3\,4\,5\,3\,4)$

TABLE 3. S-branches of χ_A.

Consider now the subspaces of $\mathbb{R}^6$

$$H = \{x \in \mathbb{R}^6 \ : \ \sum_{i=1}^{6} x_i = 1\} \ \text{ and } \ H_0 = \{x \in \mathbb{R}^6 \ : \ \sum_{i=1}^{6} x_i = 0\}.$$

For the given matrix A, its null space $\mathrm{Ker}(A)$ has dimension 2. Take a non-zero vector $w \in \mathrm{Ker}(A) \cap H_0$. The set of equilibria of the natural extension of X_A to the affine hyperplane H is

$$\mathrm{Eq}(X_A) = \mathrm{Ker}(A) \cap H = \{q + tw \colon t \in \mathbb{R}\}.$$

The Hamiltonian of X_A is the function $h_q : \Delta^5 \to \mathbb{R}$

$$h_q(x) := \sum_{i=1}^{6} q_i \log x_i,$$

where q_i is the i-th component of the equilibrium point q. Another integral of motion of X_A is the function $h_w : \Delta^5 \to \mathbb{R}$

$$h_w(x) := \sum_{i=1}^{6} w_i \log x_i \,,$$

where w_i is the i-th component of w, which is a Casimir of the underlying Poisson structure.

The skeletons of h_q and h_w are respectively $\eta_q, \eta_w : \mathcal{C}^*(\Delta^5) \to \mathbb{R}$,

$$\eta_q(y) := \sum_{i=1}^{6} q_i y_i \quad \text{and} \quad \eta_w(y) := \sum_{i=1}^{6} w_i y_i \,,$$

which we use to define $\eta : \mathcal{C}^*(\Delta^5) \to \mathbb{R}^2$, $\eta(y) := (\eta_q(y), \eta_w(y))$.

Consider the skeleton flow map $\pi_S : \Pi_S \to \Pi_S$ of χ_A, see Definition 5.9. Notice that $\Pi_S = \Pi_{\gamma_6} \cup \Pi_{\gamma_{10}}$, where by Proposition 5.10 $\Pi_{\gamma_6} = \Pi_{\xi_1} \cup \Pi_{\xi_2}$ (mod 0) and $\Pi_{\gamma_{10}} = \Pi_{\xi_3} \cup \Pi_{\xi_4} \cup \Pi_{\xi_5}$ (mod 0). By Proposition 7.2, the function η is invariant under π_S. For all $i = 1, \ldots, 5$, the polyhedral cone Π_{ξ_i} has dimension 4. Hence, each polytope $\Delta_{\xi_i,c} := \Pi_{\xi_i} \cap \eta^{-1}(c)$ is a 2-dimensional polygon.

By invariance of η, the set $\Delta_{S,c}$ is also invariant under π_S. Consider now the restriction $\pi_{S|\Delta_{S,c}}$ of π_S to $\Delta_{S,c}$. This is a piecewise affine area preserving map, see Remark 7.6. Figure 14 shows the domain $\Delta_{S,c}$ and 10 000 iterates by π_S of a point in $\Delta_{S,c}$. Following the itinerary of a random point we have picked the following heteroclinic cycle consisting of 11 S-branches

$$\xi := (\xi_1, \xi_2, \xi_4, \xi_2, \xi_4, \xi_2, \xi_4, \xi_2, \xi_4, \xi_2, \xi_4) \,.$$

The map π_ξ is represented by the matrix, see definitions (5.3) and (5.5),

$$M_\xi = \begin{pmatrix} -10 & -5 & 0 & 6 & 1 & -\frac{10}{3} \\ 0 & 0 & 0 & 0 & 0 & 0 \\ 0 & 0 & 0 & 0 & 0 & 0 \\ 1 & 1 & 0 & 0 & 0 & \frac{2}{3} \\ 10 & 5 & 1 & -5 & 0 & \frac{8}{3} \\ -\frac{3}{2} & 0 & 0 & \frac{3}{2} & 0 & 0 \end{pmatrix} \,.$$

The eigenvalues of M_ξ, besides 0 and 1 (both with geometric multiplicity 2), are (approximately)

$$\lambda_u = -11.9161, \quad \text{and} \quad \lambda_s = -0.0839202 \,.$$

The corresponding eigenvectors are

$$w_u = (-0.734728, 0., 0., 0.067307, 0.667421, -0.10096) \,,$$

$$w_s = (0.328842, 0., 0., 0.358966, -0.687808, -0.538449) \,.$$

An eigenvector associated to the eigenvalue 1 is

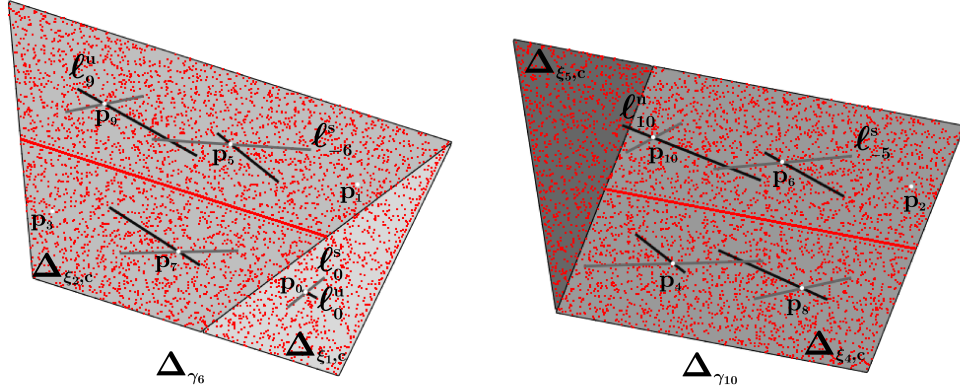$$\mathbf{p_0} = (0.20512, 0, 0, 0.325586, 0.905134, 0.180699) \,.$$

FIGURE 14.   Homoclinic intersections for the periodic
orbit of $\mathbf{p_0}$ under the area preserving map $\pi_{S|\Delta_{S,c}}$.

Notice that this $\mathbf{p_0}$ is not unique because $\dim(\mathrm{Ker}(M_\xi - I)) = 2$. We
have chosen $c := (c_1, c_2) = (0.343447, -0.242852)$ so that $\eta(\mathbf{p_0}) = c$,
i.e., $\mathbf{p_0} \in \Delta_{S,c}$. In fact we have $\mathbf{p_0} \in \Delta_{\xi_1,c} \subset \Delta_{\gamma_6,c}$. Hence $\mathbf{p_0}$ is a
periodic point of the skeleton flow map π_S with period 11.

Figure 14 also depicts the polygons $\Delta_{\xi_1,c}, \Delta_{\xi_2,c}$ contained in Δ_{γ_6}, and
$\Delta_{\xi_4,c}, \Delta_{\xi_5,c}$ contained in $\Delta_{\gamma_{10}}$. The set $\Delta_{\xi_3,c}$ is empty for this choice of
c. The orbit of $\mathbf{p_0}$ is represented by the white dots in Figure 14.

Let ℓ_0^u and ℓ_0^s be line segments through $\mathbf{p_0}$, contained in $\Delta_{\xi_1,c}$, re-
spectively aligned with the eigen-directions w_s and w_u. We denote by
ℓ_n^u the n-th forward π_S-iterate of ℓ_0^u and by ℓ_{-m}^s the m-th backward
π_S-iterate of ℓ_0^s, *i.e.*,

$$\ell_n^u := \pi_S^n(\ell_0^u) \quad \text{and} \quad \ell_{-m}^s := \pi_S^{-m}(\ell_0^s).$$

Let $\mathbf{p_k} = \pi_S^k(\mathbf{p_0})$ and notice that $\mathbf{p_{10}} = \pi_S^{10}(\mathbf{p_0}) = \pi_S^{-1}(\mathbf{p_0}) = \mathbf{p_{-1}}$.
Figure 14 also shows that in a few iterates transversal intersections
occur between the "local stable" and the "local unstable" manifolds of
different points of the periodic orbit of $\mathbf{p_0}$. Namely, $\ell_{-6}^s \cap \ell_9^u \neq \emptyset$ and
$\ell_{-5}^s \cap \ell_{10}^u \neq \emptyset$.

By Theorem 7.8 this implies the existence of chaotic behavior for
the flow of X_A in some level set $h_q^{-1}(c_1/\epsilon) \cap h_w^{-1}(c_2/\epsilon)$, with $c = (c_1, c_2)$
chosen above and for all small enough $\epsilon > 0$.

9.2. **Example 2.** Consider the replicator system defined by matrix

$$B = \begin{pmatrix} 0 & 1 & -2 & 0 & 2 & -1 \\ -1 & 0 & 1 & -2 & 0 & 2 \\ 2 & -1 & 0 & 1 & -2 & 0 \\ 0 & 2 & -1 & 0 & 1 & -2 \\ -2 & 0 & 2 & -1 & 0 & 1 \\ 1 & -2 & 0 & 2 & -1 & 0 \end{pmatrix}.$$

We denote by X_B the vector field associated to this replicator defined on the simplex Δ^5. The point

$$q = \left(\frac{1}{6}, \frac{1}{6}, \frac{1}{6}, \frac{1}{6}, \frac{1}{6}, \frac{1}{6} \right) \in \mathbb{R}^6$$

is an equilibrium of the replicator X_B. Since matrix B is skew-symmetric, the associated replicator is conservative, *i.e.*, X_B is Hamiltonian with respect to some stratified Poisson structure on Δ^5.

Using the notation of the previous example, the skeleton character χ_B of X_B is displayed in Table 4. This model has 15 edges: 3 neutral edges, γ_3, γ_8, γ_{12}, and 12 flowing-edges, γ_1, γ_2, γ_4, γ_5, γ_6, γ_7, γ_9, γ_{10}, γ_{11}, γ_{13}, γ_{14}, γ_{15}. The flowing-edge directed graph of χ is represented in Figure 15.

χ_σ^v	σ_1	σ_2	σ_3	σ_4	σ_5	σ_6
v_1	0	1	−2	0	2	−1
v_2	−1	0	1	−2	0	2
v_3	2	−1	0	1	−2	0
v_4	0	2	−1	0	1	−2
v_5	−2	0	2	−1	0	1
v_6	1	−2	0	2	−1	0

TABLE 4. The skeleton character of X_B.

From this graph we can see that

$$S = \{ \gamma_1 = (1\,2),\ \gamma_4 = (1\,5),\ \gamma_7 = (2\,4),\ \gamma_{10} = (5\,4) \}$$

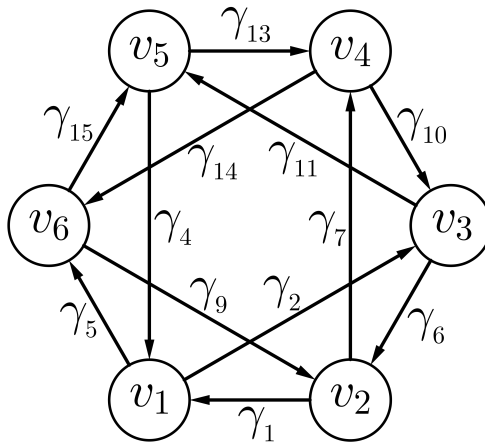is a structural set for χ_B, whose S-branches denoted by $\xi_1, \ldots, \xi_{32}$ are displayed in Table 5.

FIGURE 15. The oriented graph of χ.

From\To	$\gamma_1 = (2\,1)$	$\gamma_4 = (5\,1)$	$\gamma_7 = (2\,4)$	$\gamma_{10} = (5\,4)$
$\gamma_1 = (2\,1)$	$\xi_1 = (2\,1\,3\,2\,1)$ $\xi_2 = (2\,1\,6\,2\,1)$	$\xi_3 = (2\,1\,3\,5\,1)$ $\xi_4 = (2\,1\,6\,5\,1)$	$\xi_5 = (2\,1\,3\,2\,4)$ $\xi_6 = (2\,1\,6\,2\,4)$	$\xi_7 = (2\,1\,3\,5\,4)$ $\xi_8 = (2\,1\,6\,5\,4)$
$\gamma_4 = (5\,1)$	$\xi_9 = (5\,1\,3\,2\,1)$ $\xi_{10} = (5\,1\,6\,2\,1)$	$\xi_{11} = (5\,1\,3\,5\,1)$ $\xi_{12} = (5\,1\,6\,5\,1)$	$\xi_{13} = (5\,1\,3\,2\,4)$ $\xi_{14} = (5\,1\,6\,2\,4)$	$\xi_{15} = (5\,1\,3\,5\,4)$ $\xi_{16} = (5\,1\,6\,5\,4)$
$\gamma_7 = (2\,4)$	$\xi_{17} = (2\,4\,3\,2\,1)$ $\xi_{18} = (2\,4\,6\,2\,1)$	$\xi_{19} = (2\,4\,3\,5\,1)$ $\xi_{20} = (2\,4\,6\,5\,1)$	$\xi_{21} = (2\,4\,3\,2\,4)$ $\xi_{22} = (2\,4\,6\,2\,4)$	$\xi_{23} = (2\,4\,3\,5\,4)$ $\xi_{24} = (2\,4\,6\,5\,4)$
$\gamma_{10} = (5\,4)$	$\xi_{25} = (5\,4\,3\,2\,1)$ $\xi_{26} = (5\,4\,6\,2\,1)$	$\xi_{27} = (5\,4\,3\,5\,1)$ $\xi_{28} = (5\,4\,6\,5\,1)$	$\xi_{29} = (5\,4\,3\,2\,4)$ $\xi_{30} = (5\,4\,6\,2\,4)$	$\xi_{31} = (5\,4\,3\,5\,4)$ $\xi_{32} = (5\,4\,6\,5\,4)$

TABLE 5. S-branches of χ.

Consider the affine subspaces $H, H_0 \subset \mathbb{R}^6$ of the previous example. For the given matrix B, its null space $\mathrm{Ker}(B)$ has dimension 2. Take a non-zero vector $w \in \mathrm{Ker}(B) \cap H_0$. As before, $\{q + tw \colon t \in \mathbb{R}\}$ is the set of equilibria of X_B on the affine hyperplane H. The same functions h_q and h_w are respectively the Hamiltonian and an integral of motion. The skeletons of these functions are respectively η_q and η_w, which we take as the components of a piecewise linear function $\eta \colon \mathcal{C}^*(\Delta^5) \to \mathbb{R}^2$. By Proposition 7.2, η is invariant under π_S. The map π_S acts on $\Pi_S = \Pi_{\gamma_1} \cup \Pi_{\gamma_4} \cup \Pi_{\gamma_7} \cup \Pi_{\gamma_{10}}$, where

- $\Pi_{\gamma_1} = \Pi_{\xi_1} \cup \Pi_{\xi_2} \cup \cdots \cup \Pi_{\xi_8} \pmod{0}$,
- $\Pi_{\gamma_4} = \Pi_{\xi_9} \cup \Pi_{\xi_{10}} \cup \cdots \cup \Pi_{\xi_{16}} \pmod{0}$,
- $\Pi_{\gamma_7} = \Pi_{\xi_{17}} \cup \Pi_{\xi_{18}} \cup \cdots \cup \Pi_{\xi_{24}} \pmod{0}$,
- $\Pi_{\gamma_{10}} = \Pi_{\xi_{25}} \cup \Pi_{\xi_{26}} \cup \cdots \cup \Pi_{\xi_{32}} \pmod{0}$.

For all $i = 1, \ldots, 32$, the polyhedral cone Π_{ξ_i} has dimension 4 while $\Delta_{\xi_i,c}$ is a 2-dimensional polygon. The 2-dimensional level set $\Delta_{S,c}$ is invariant under π_S and we denote by $\pi_{S|\Delta_{S,c}}$ the restriction of π_S to $\Delta_{S,c}$. Figure 16 shows the domain $\Delta_{S,c}$ and $25\,000$ iterates by π_S of a point in $\Delta_{S,c}$ with random like distribution. Following the itinerary of a random point we have picked a heteroclinic cycle ξ consisting of 13 S-branches

$$\xi := (\xi_{31}, \xi_{32}, \xi_{32}, \xi_{28}, \xi_{12}, \xi_{10}, \xi_2, \xi_1, \xi_5, \xi_{21}, \xi_{21}, \xi_{23}, \xi_{31}).$$

The skeleton flow map π_ξ is represented by the matrix

$$M_\xi = \begin{pmatrix} 1 & \frac{3}{2} & \frac{51}{8} & -\frac{35}{4} & -\frac{33}{8} & -\frac{15}{4} \\ 0 & -\frac{1}{2} & -\frac{21}{8} & \frac{21}{4} & \frac{23}{8} & \frac{9}{4} \\ 0 & -\frac{3}{2} & -\frac{43}{8} & \frac{35}{4} & \frac{41}{8} & \frac{15}{4} \\ 0 & 0 & 0 & 0 & 0 & 0 \\ 0 & 0 & 0 & 0 & 0 & 0 \\ 0 & \frac{3}{2} & \frac{21}{8} & -\frac{17}{4} & -\frac{23}{8} & -\frac{5}{4} \end{pmatrix}.$$

The eigenvalues of M_ξ, besides 0 and 1 (both with geometric multiplicity 2), are

$$\lambda_u = -8, \quad \text{and} \quad \lambda_s = -\frac{1}{8}.$$

The corresponding eigenvectors are

$$w_u = (2, -1, -2, 0, 0, 1),$$
$$w_s = (-1, -1, 1, 0, 0, 1).$$

An eigenvector associated to the eigenvalue 1 is

$$\mathbf{p_0} = (0.62, 0.304, 0.152, 0, 0, 0.38).$$

Notice that this $\mathbf{p_0}$ is not unique because $\dim(\text{Ker}(M_\xi - I)) = 2$. We have chosen $c := (c_1, c_2) = (0.242667, -0.088)$ so that $\eta(\mathbf{p_0}) = c$, *i.e.*, $\mathbf{p_0} \in \Delta_{S,c}$. In fact we have $\mathbf{p_0} \in \Delta_{\xi_{31},c} \subset \Delta_{\gamma_{10},c}$. Hence $\mathbf{p_0}$ is a periodic point of the skeleton flow map π_S with period 13.

Figure 16 also depicts the polygons $\Delta_{\xi_1,c}, \Delta_{\xi_2,c}, \Delta_{\xi_5,c}$ contained in Δ_{γ_1}, $\Delta_{\xi_{10},c}, \Delta_{\xi_{11},c}, \Delta_{\xi_{12},c}$ contained in Δ_{γ_4}, $\Delta_{\xi_{21},c}, \Delta_{\xi_{22},c}, \Delta_{\xi_{23},c}$ contained in Δ_{γ_7} and $\Delta_{\xi_{28},c}, \Delta_{\xi_{31},c}, \Delta_{\xi_{32},c}$ contained in $\Delta_{\gamma_{10}}$. The remaining sets $\Delta_{\xi_i,c}$ are empty for this choice of c. The orbit of $\mathbf{p_0}$ is represented by the white dots in Figure 16.

Let ℓ_n^u and ℓ_{-m}^s denote the stable and unstable local manifolds along the orbit of $\mathbf{p_0}$, the notation introduced in the previous example. Write $\mathbf{p_k} = \pi_S^k(\mathbf{p_0})$ and notice that $\mathbf{p_{12}} = \pi_S^{12}(\mathbf{p_0}) = \pi_S^{-1}(\mathbf{p_0}) = \mathbf{p_{-1}}$.

Figure 16 also shows that in the first forward and backward iterate (by the skeleton flow map) transversal intersections occur between the "local stable" and the "local unstable" manifolds of different points of the periodic orbit of $\mathbf{p_0}$. Namely, $\ell_1^u \cap \ell_0^s \neq \emptyset$, $\ell_{-1}^s \cap \ell_0^u \neq \emptyset$ and $\ell_1^u \cap \ell_{-1}^s \neq \emptyset$.

By Theorem 7.8 this implies the existence of chaotic behavior for the flow of the replicator X_B.

10. Conclusions and furtherwork

For the Hamiltonian polymatrix replicator systems, alluded in Remark 7.5 and studied in [1] by the first two authors, their invariant algebraic Poisson structures induce stratified piecewise constant Poisson structures on the dual cone, preserved by the corresponding skeleton flow. In other words, the skeleton flow inherits the conservative Hamiltonian nature of the original polymatrix replicator vector field. This subject will be addressed by the authors in a future work. Remark 7.6 follows from this theory.

In the Hamiltonian examples discussed in Section 9, chaotic (hyperbolic) and regular (elliptic) behavior co-exist. In both of them, the skeleton flow maps are piecewise linear area preserving maps. Example 2 exhibits a few elliptic periodic points surrounded by invariant curves that we will refer to as *elliptic domains*[5], see Figure 16. Notice how the invariant curves break up as they touch the boundary of the associated domain $\Delta_{\xi,c}$. Outside these elliptic domains, a chaotic sea

---

[5] These are not KAM islands because the piecewise linearity of π_S does not allow any twist.
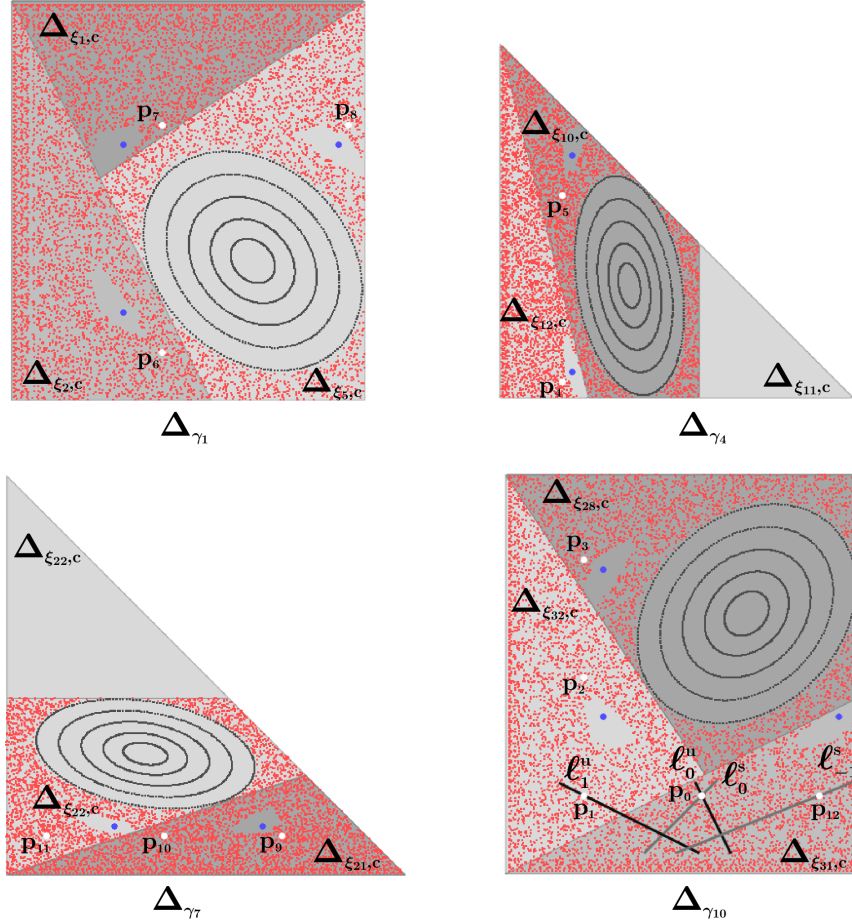
FIGURE 16. Homoclinic intersections for the periodic orbit of $\mathbf{p_0}$ under the area preserving map $\pi_{S|\Delta_{S,c}}$.

('random' orbits with positive Lyapunov exponents) seems to prevail. In Figure 16 we can also see a couple of triangular components, $\Delta_{\xi_{11},c}$, $\Delta_{\xi_{22},c}$, consisting of π_S-fixed points and 10 cyclically permuted small islands each being a *continuum* of periodic points. These examples solicit the development of an ergodic theory for the class of piecewise linear area preserving maps, and more generally for the class of piecewise linear symplectic maps. We mention a few natural questions about the generic behavior of these systems: *Can the number of elliptic domains be infinite? Is the complement of the elliptic domains non-uniformly hyperbolic with respect to Lebesgue measure? Is this complement typically ergodic? Can it have infinitely many ergodic components?* In the context of smooth area preserving maps these are very hard open problems, but due to their dynamical rigidity these sort of problems might be much more feasible for piecewise linear area preserving maps. Such a theory would provide a good insight on the asymptotic dynamics

(along the vertex-edge network) for the classes of Hamiltonian systems on polytopes mentioned above.

General vector fields $X \in \mathfrak{X}^\omega(\Gamma^d)$ typically do not have any integral of motion and the analysis of their dynamics must be different from the conservative case. The skeleton flow map $\pi_S : \Pi_S \to \Pi_S$ can be projectivized as follows. Take $\eta : \mathcal{C}^*(\Gamma^d) \to \mathcal{R}$ to be the piecewise linear function $\eta(y) := \sum_{\sigma \in F} y_\sigma$ and define $\Delta_\gamma := \Pi_\gamma \cap \eta^{-1}(1)$, $\Delta_\xi := \Pi_\xi \cap \eta^{-1}(1)$ as before. The simplex Δ_γ can be viewed as the projectivization of the sector Π_γ because every half-line through the origin in Π_γ intersects Δ_γ at a single point. Likewise Δ_ξ is the projectivization of Π_ξ. If ξ is a heteroclinic path ending at some flowing edge γ then the linear map $\pi_\xi : \Pi_\xi \to \Pi_\gamma$ induces a projective map $\hat{\pi}_S : \Delta_\xi \to \Delta_\gamma$ defined by $\hat{\pi}_\xi(y) := \eta(\pi_\xi(y))^{-1}\pi_\xi(y)$. These are the branches of the *projective skeleton map* $\hat{\pi}_S : \Delta_S \to \Delta_S$ defined on $\Delta_S := \cup_{\xi \in \mathscr{B}(\chi)}\Delta_\xi$ by $\hat{\pi}_S(y) := \hat{\pi}_\xi(y)$ if $y \in \Delta_\xi$ for some S-branch ξ. The suspension of the projective map $\hat{\pi}_S$ on Δ_S can be viewed as a *blowup* of the flow φ_X^t along the polytope's boundary, *i.e.*, $\hat{\pi}_S$ extends the dynamics of φ_X^t to the *blown-up* polytope's boundary. In the conservative case, if $h \in \mathcal{H}(\Gamma^d)$ is a proper X-invariant function with skeleton η and the same order function as X, the projective skeleton map $\hat{\pi}_S$ rules the common dynamics on all level sets of η.

The map π_S factors through $\hat{\pi}_S$ acting linearly on the fibers. Hence π_S may be regarded as a 1-dimensional linear cocycle over $\hat{\pi}_S$, where the sign of its Lyapunov exponent gives the repelling *vs* attracting nature of the asymptotic boundary dynamics. Given a heteroclinic cycle ξ, if $v \in \Delta_\xi$ is an eigenvector of M_ξ with a positive eigenvalue then v is a periodic point of $\hat{\pi}_S$ whose nature can be read from the spectrum of M_ξ. This spectrum also determines whether the heteroclinic cycle ξ is attracting or repelling. If a compact $\hat{\pi}_S$-invariant set is partially hyperbolic (with a central direction of co-dimension 1) regarded as an invariant subset of the blown-up boundary of the flow φ_X^t then it determines a local strong stable/unstable foliation in the polytope's interior. The special case where this compact invariant set is a single periodic orbit provides an invariant (local stable/unstable) manifold of the heteroclinic cycle associated with the periodic orbit. These dynamical foliations and invariant manifolds are useful tools to analyze the dynamics in the polytope's interior, part of a theory being developed in a work under preparation. This theory could for instance help to provide sufficient conditions for permanence, an important concept in EGT. In this spirit, a theorem of Jansen [13] with a game flavored sufficient criteria for permanence, in the framework of replicator dynamics, was recently extended by the third author to the broader class of polymatrix replicators [15].

Although the piecewise linear maps π_S are in general discontinuous, because orbits in adjacent domains eventually diverge, in some cases

π_S is continuous throughout several neighboring domains. This implies that the rescaling along the vertex-edge polytope' skeleton can be augmented to include some higher dimensional faces of the polytope. An extreme example is the 3-dimensional Hamiltonian depicted in Figure 6, which has a globally continuous skeleton flow. In this model the rescaling can be augmented to include the whole cube's boundary. This will the subject of another future work.

This theory can be applied to most ODE models in EGT. For systems depending on many parameters, an algorithmic analysis of the skeleton (asymptotic) dynamics can split the space of parameters into regions where the dynamics of the skeleton flow maps are qualitatively similar. This would help to understand the bifurcations taking place in the polytope's interior as the parameters cross the boundary between adjacent regions. For example, higher dimensional cases of the systems studied at [21] could be investigated. In each parametric region, the mentioned tools can be used to detect and characterize some of its invariant dynamical structures such as heteroclinic cycles, periodic points, hyperbolic invariant sets, invariant manifolds and invariant foliations, which are essential to understand the model's dynamics in the polytope's interior. In some future work the authors plan to illustrate this approach with the analysis of some concrete EGT model.

Acknowledgments

References

[1] Hassan Najafi Alishah and Pedro Duarte, *Hamiltonian evolutionary games*, J. Dyn. Games **2** (2015), no. 1, 33–49. MR3370936

[2] Hassan Najafi Alishah, Pedro Duarte, and Telmo Peixe, *Conservative and dissipative polymatrix replicators*, J. Dyn. Games **2** (2015), no. 2, 157–185. MR3436357

[3] W Brannath, *Heteroclinic networks on the tetrahedron*, Nonlinearity **7** (1994), no. 5, 1367.

[4] L. A. Bunimovich and B. Z. Webb, *Isospectral compression and other useful isospectral transformations of dynamical networks*, Chaos: An Interdisciplinary Journal of Nonlinear Science **22** (2012), no. 3, –.

[5] Tsuyoshi Chawanya, *A new type of irregular motion in a class of game dynamics systems*, Progr. Theoret. Phys. **94** (1995), no. 2, 163–179. MR1354590 (96f:58142)

[6] ———, *Infinitely many attractors in game dynamics system*, Progr. Theoret. Phys. **95** (1996), no. 3, 679–684. MR1388249

[7] Pedro Duarte, *Hamiltonian systems on polyhedra*, Dynamics, games and science. II, 2011, pp. 257–274. MR2883285

[8] Pedro Duarte and Telmo Peixe, *Flows on polytopes (mathematica code)*.

[9] Michael Field, *Lectures on bifurcations, dynamics and symmetry*, Pitman Research Notes in Mathematics Series, vol. 356, Longman, Harlow, 1996. MR1425388

[10] Josef Hofbauer, *Heteroclinic cycles on the simplex*, Proceedings of the Eleventh International Conference on Nonlinear Oscillations (Budapest, 1987), 1987, pp. 828–831. MR933673 (89e:58099)

[11] ———, *Heteroclinic cycles in ecological differential equations*, Tatra Mt. Math. Publ. **4** (1994), 105–116. Equadiff 8 (Bratislava, 1993). MR1298459 (95i:34083)

[12] Josef Hofbauer and Karl Sigmund, *Evolutionary games and population dynamics*, Cambridge University Press, Cambridge, 1998. MR1635735

[13] Wolfgang Jansen, *A permanence theorem for replicator and Lotka-Volterra systems*, J. Math. Biol. **25** (1987), no. 4, 411–422. MR908382 (89a:92044)

[14] Vivien Kirk and Mary Silber, *A competition between heteroclinic cycles*, Nonlinearity **7** (1994), no. 6, 1605–1621. MR1304441 (95j:58121)

[15] Telmo Peixe, *Permanence in polymatrix replicators*. To appear.

[16] Peter Schuster and Karl Sigmund, *Coyness, philandering and stable strategies*, Animal Behaviour **29** (1981), no. 1, 186 –192.

[17] Peter Schuster, Karl Sigmund, Josef Hofbauer, and Robert Wolff, *Self-regulation of behaviour in animal societies. II. Games between two populations without self-interaction*, Biol. Cybernet. **40** (1981), no. 1, 9–15. MR609926 (82e:92039b)

[18] Leonid P. Shilnikov, Andrey L. Shilnikov, Dmitry V. Turaev, and Leon O. Chua, *Methods of qualitative theory in nonlinear dynamics. Part I*, World Scientific Series on Nonlinear Science. Series A: Monographs and Treatises, vol. 4, World Scientific Publishing Co., Inc., River Edge, NJ, 1998. With the collaboration of Sergey Gonchenko (Sections 3.7 and 3.8), Oleg Sten′kin (Section 3.9 and Appendix A) and Mikhail Shashkov (Sections 6.1 and 6.2). MR1691840

[19] Michael Shub, *Global stability of dynamical systems*, Springer-Verlag, New York, 1987. With the collaboration of Albert Fathi and Rémi Langevin, Translated from the French by Joseph Christy. MR869255 (87m:58086)

[20] Peter D. Taylor and Leo B. Jonker, *Evolutionarily stable strategies and game dynamics*, Math. Biosci. **40** (1978), no. 1-2, 145–156. MR0489983 (58 #9351)

[21] Yuanshi Wang, Hong Wu, and Shigui Ruan, *Periodic orbits near heteroclinic cycles in a cyclic replicator system*, J. Math. Biol. **64** (2012), no. 5, 855–872. MR2910794

[22] Günter M. Ziegler, *Lectures on polytopes*, Graduate Texts in Mathematics, vol. 152, Springer-Verlag, New York, 1995. MR1311028

Departamento de Matemática, Instituto de Ciências Exatas, Universidade Federal de Minas Gerais, Belo Horizonte, 31270-901, Brazil
  E-mail address: halishah@mat.ufmg.br

Departamento de Matemática and CMAF, Faculdade de Ciências, Universidade de Lisboa, Campo Grande, Edificio C6, Piso 2, 1749-016 Lisboa, Portugal
  E-mail address: pmduarte@fc.ul.pt

REM and CEMAPRE, ISEG Lisbon School of Economics & Management, Universidade de Lisboa, Rua do Quelhas, 6, 1200-781 Lisboa, Portugal
  E-mail address: telmop@iseg.ulisboa.pt